Supporting Information

Vitex negundo-Fe_3O_4-CuO green nanocatalyst (*VN*-Fe_3O_4-CuO): Synthesis of the antimicrobial activity of pyrazolo[3,4-c]pyrazole derivatives via cyclization of isoniazid with pyrazole and their investigation cytotoxicity and molecular docking studies

Idhayadhulla Akbar,[*a] Janani Mullaivendhan [a], Anis Ahamed [b] and Hossam M. Aljawdah[c]

[a]Research Department of Chemistry, Nehru Memorial College (Affiliated Bharathidasan University), Puthanampatti-621007, Tamilnadu, India;

[b]Department of Botany and Microbiology, College of science, King Saud University, P.O. Box 2455, Riyadh 11451, Saudi Arabia.

[c]Department of Zoology, College of Science, King Saud University, P.O. Box 2455, Riyadh 11451, Saudi Arabia;

Correspondence: a.idhayadhulla@gmail.com;

Experimental Section

2. Materials and Methods

2.3.1. Synthesis of (3-(4-Chlorophenyl)-4-methyl-6-phenyl pyrazolo[3,4-c]pyrazol-2(1*H*,3*H*,6*H*)-yl)(pyridin-4-yl)methanone (1a)

Light Yellow solid; Yield: 82%; (8.702mg; M.p. 141–143°C); IR(KBr) ν: 3323, 2974, 1655, 1640cm^{-1}; ^{1}H NMR(DMSO-d$_6$, 300 MHz): δ 8.36 (2H, d, *J* = 6.23 Hz, -Pyridin), 7.83 (-Pyridin, 2H, d, *J* = 6.22 Hz), 7.58 (5H, -Ar ring, t, *J* = 6.21 Hz), 7.30 (5H, m, -Ar ring), 6.13 (s, 1H, -CH), 4.0 (1H, s, -NH), 1.97 (s, 3H, -CH$_3$); ^{13}C NMR (DMSO-d$_6$, 75 MHz): δ 172.0 (C=O, 1C), 149.0-105.7 (-1C, 3C), 149.7-121.7 (5C, -pyridine), 142.8-123.9 (12C, -Ar ring), 68.1 (1C, -CH), 12.7 (1C, -CH$_3$); EI-MS, m/z: 381.43 (M$^+$, 26.8%); Anal. calcd. for (C$_{23}$H$_{19}$N$_5$O): C, 72.42; H, 5.02; N, 18.36%; Found: C, 72.43; H, 5.00, N, 18.30%.

2.4.2. (3-(4-Chlorophenyl)-4-methyl-6-phenylpyrazolo[3,4-c]pyrazol-2(1*H*,3*H*,6*H*)-yl)(pyridin-4-yl)methanone (1b)

Yellow solid; Yield: 81%; (11.382 mg); M.p. 167–165°C; IR(KBr) ν: 3323, 2974, 1655, 1640cm^{-1}; ^{1}H NMR(DMSO-d$_6$, 300 MHz): δ 8.36 (-Pyridin, d, *J* = 6.23 Hz, 2H), 7.83 (-Pyridin, 2H, d, *J* = 6.22 Hz), 7.58 (5H, -Ar ring, t, *J* = 6.21 Hz), 7.34 (-Ar ring, 4H, dd, *J* = 7.33 Hz, *J* = 7.37 Hz), 6.23 (s, 1H, -CH), 4.0 (1H, s, -NH), 1.97 (3H, s, -CH$_3$); ^{13}C NMR (DMSO-d$_6$, 75 MHz): δ 172.0 (C=O, 1C), 145.8 (-C, 3C), 149.7-121.7 (-pyridine, 5C), 140.8-123.9 (12C, -Ar ring), 68.1 (1C, -CH), 12.7 (-CH$_3$, 1C); EI-MS, m/z: 415.87 (M$^+$, 32.6%); Anal. calcd. for (C$_{23}$H$_{18}$ClN$_5$O): C, 66.45; H, 4.33; N, 16.81%; Found: C, 66.41; H, 4.32; N, 16.83%.

2.4.3. (3-(4-Hydroxyphenyl)-4-methyl-6-phenylpyrazolo[3,4-c]pyrazol-2(1*H*,3*H*,6*H*)-yl)(pyridin-4-yl)methanone (1c)

White solid; Yield: 69%; (8.426mg; M.p. 176–178°C); IR(KBr) ν: 3323, 2974, 1655, 1640cm^{-1}; ^{1}H NMR(DMSO-d$_6$, 300 MHz): δ 8.36 (-Pyridin, 2H, d, *J* = 6.23 Hz), 7.82 (-Pyridin, d, *J* = 6.22 Hz, 2H), 7.60 (2H, -Ar ring, d, *J* = 6.21 Hz), 6.40 (2H, d, *J* = 6.23 Hz, -Ar ring), 7.58 (5H, t, *J* = 6.21 Hz, -Ar ring), 6.12 (1H, -CH, s), 5.35 (s, -OH, 1H), 4.0 (s, -NH, 1H), 1.97 (s, 3H, -CH$_3$); ^{13}C NMR (DMSO-d$_6$, 75 MHz): δ

172.0 (1C, C=O), 149.7-105.7 (3C, -C), 149.7-121.7 (5C, -pyridine), 156.2-115.2 (12C, -Ar ring), 68.1 (-CH, 1C), 12.7 (-CH_3, 1C); EI-MS, m/z: 397.43(M^+, 25.2%); Anal. calcd. for ($C_{23}H_{19}N_5O_2$): C, 69.51; H, 4.82; N, 17.62%; Found: C, 69.57; H, 4.81; N, 17.66%.

2.4.4. (4-methyl-3-(4-nitrophenyl)-6-phenylpyrazolo[3,4-c]pyrazol-2(1*H*,3*H*,6*H*)-yl)(pyridin-4-yl)methanone (1d)

Light Yellow solid; Yield: 80%; (10.971mg; M.p. 157–159°C); IR(KBr) ν: 3323, 2974, 1655, 1640cm^{-1}; ^{1}H NMR(DMSO-d_6, 300 MHz): δ 8.36 (-Pyridin, 2H, d, *J* = 6.23 Hz), 7.85 (-Pyridin, 2H, d, *J* = 6.22 Hz), 7.34 (-Ar ring, 4H, dd, *J* = 7.33 Hz, *J* = 7.37 Hz), 7.58 (5H, t, *J* = 6.21 Hz, -Ar ring), 6.13 (s, 1H, -CH), 4.0 (1H, s, -NH), 1.97 (s, 3H, -CH_3); ^{13}C NMR (DMSO-d_6, 75 MHz): δ 172.0 (C=O, 1C), 145.8 (3C, -C), 149.7-121.7 (5C, -pyridine), 148.2-123.9 (12C, -Ar ring), 68.1 (1C, -CH), 12.7 (-CH_3, 1C); EI-MS, m/z: 426.43 (M^+, 25.2 %); Anal. calcd. for: ($C_{23}H_{18}N_6O_3$): C, 64.78; H, 4.25; N, 19.71%; Found: C, 64.76; H, 4.26; N, 19.74%.

2.4.5. (3-(4-Methoxyphenyl)-4-methyl-6-phenylpyrazolo[3,4-c]pyrazol-2(1*H*,3*H*,6*H*)-yl)(pyridin-4-yl)methanone (1e)

Light Yellow solid; Yield: 79%; (10.755mg; M.p. 173–175°C); mw189; IR(KBr) ν: 3323, 2974, 1655, 1640cm^{-1}; ^{1}H NMR(DMSO-d_6, 300 MHz): δ 8.36 (-Pyridin, 2H, d, *J* = 6.23 Hz), 7.83 (-Pyridin, 2H, d, *J* = 6.22 Hz), 7.15 (4H, -Ar ring, dd, *J* = 7.33 Hz, *J* = 7.37 H), 7.58 (5H, -Ar ring, t, *J* = 6.21 Hz), 6.13 (-CH, s, 1H), 4.0 (-NH, s, 1H), 3.89 (3H, -CH_3, s), 1.97 (s, 3H, -CH_3); ^{13}C NMR (DMSO-d_6, 75 MHz): δ 172.0 (1C, C=O), 145.8 (3C, -C), 149.7-121.7 (5C, -pyridine), 158.7-114.1 (12C, -Ar ring), 68.1 (1C, -CH), 55.12 (1C, -CH_3), 12.7 (1C, -CH_3); EI-MS, m/z: 411.46 (M^+, 27.9%); Anal. calcd. for ($C_{24}H_{21}N_5O_2$): C, 70.06; H, 5.14; N, 17.02%; Found: C, 70.04; H, 5.13; N, 17.01%.

2.4.6. (3-(4-(Dimethylamino)phenyl)-4-methyl-6-phenyl pyrazolo[3,4-c]pyrazol-2(1*H*,3*H*,6*H*)-yl)(pyridin-4-yl) methanone (1f)

Yellow solid; Yield: 75%; (10.285mg); M.p. 161–164°C; IR(KBr) ν: 3323, 2971, 1655, 1640cm^{-1}; ^{1}H NMR(DMSO-d_6, 300 MHz): δ 8.36 (-Pyridin, d, *J* = 6.23 Hz,

2H), 7.69 (d, -Pyridin, 2H, *J* = 6.22 Hz), 7.0 (2H, -Ar ring, d, *J* = 6.24 Hz), 7.58 (-Ar ring, 5H, t, *J* = 6.21 Hz), 6.48 (-Ar ring, d, *J* = 6.23 Hz, 2H), 6.13 (1H, s, -CH), 4.0 (s, 1H, -NH), 3.07 (s, 6H, $-CH_3$), 1.92 (s, 3H, $-CH_3$); ^{13}C NMR (DMSO-d_6, 75 MHz): δ 191.0 (C=O, 1C), 145.8 (3C, -C), 149.7-121.7 (5C, -pyridine), 142.1-123.4 (12C, -Ar ring), 76. 1 (1C, -CH), 41.3 (2C, -C), 12.7 (1C, $-CH_3$); EI-MS, m/z: 424.50 (M^+, 29.3 %); Anal. calcd. for ($C_{25}H_{24}N_6O$): C, 70.73; H, 5.70; N, 19.80%; Found: C, 70.72; H, 5.72; N, 19.81%.

2.4.7. (3-(2,6-Dimethylhepta-1,5-dien-1-yl)-4-methyl-6-phenyl pyrazolo[3,4-c]pyrazol-2(1*H*,3*H*,6*H*)-yl)(pyridin-4-yl)methanone (1g)

Light Yellow solid; Yield: 81%; (11.108mg); M.p. 144–146°C; IR(KBr) ν: 3323, 2974, 1655, 1640cm^{-1}; ^{1}H NMR(DMSO-d_6, 300 MHz): δ 8.36 (-Pyridin, d, *J* = 6.2 Hz, 2H), 7.42 (-Ar ring, d, *J* = 6.22 Hz, 2H), 7.58 (5H, t, *J* = 6.21 Hz, -Ar ring), 5.53 (1H, d, -CH), 5.37,5.23 (2H, -H, s), 4.0 (1H, s, -NH), 2.00 (4H, CH_2), 1.97 (3H, s, $-CH_3$), 1.84 (3H, $-CH_3$, s), 1.88 (3H, s, $-CH_3$), .1.59 (3H, s, $-CH_3$); ^{13}C NMR (DMSO-d_6, 75 MHz): δ 172.0 (C=O, 1C), 145.8 (5C, -C), 149.7-121.7 (5C, -pyridine), 139.7-123.9 (6C, -Ar ring), 123.5 (1C, -CH), 61.1 (1C, -CH), 39.7 (1C, $-CH_2$), 26.4 ($-CH_2$, 1C), 116.2 (-CH, 1C), 26.7 ($-CH_3$, 1C), 18.0 ($-CH_3$, 1C), 16.1 ($-CH_3$, 1C), 12.7 ($-CH_3$, 1C); EI-MS, m/z: 427.54 (M^+, 28.5%); Anal. calcd. for ($C_{26}H_{29}N_5O$): C, 73.04; H, 6.84; N, 16.38%; Found: C, 73.05; H, 6.82, N, 16.82%.

2.4.8. (3-(1H-indol-3-yl)-4-methyl-6-phenylpyrazolo[3,4-c]pyrazol-2 (1*H*,3*H*,6*H*)-yl)(pyridin-4-yl)methanone (1h)

Yellow solid; Yield: 73%; (10.011mg); M.p. 160–163°C; IR(KBr) ν: 3323, 2972, 1651, 1643cm^{-1}; ^{1}H NMR(DMSO-d_6, 300 MHz): δ 10.1 (1H, s, -NH), 8.36 (d, -Pyridin, *J* = 6.23 Hz , 2H), 7.84 (d, *J* = 6.22 Hz, 2H, -Pyridin), 7.18 (s, -CH, 1H), 7.15 (-Ar ring, 4H, t, *J*= 6.23 Hz , *J* = 6.24 Hz), 7.58 (5H, -Ar ring, t, *J* = 6.21 Hz), 6.13 (1H, s, -CH), 4.0 (1H, s, -NH), 1.97 (s, 3H, $-CH_3$); ^{13}C NMR (DMSO-d_6, 75 MHz): δ 172.0 (C=O, 1C), 145.8 (4C, -C), 149.7-120.3 (4C, -pyridine), 123.9 (1C, $-CH_3$) 139.7-111.1 (12C, -Ar ring), 105.7 (1C, $-CH_2$), 66.1 (-CH, 1C), 12.7 (1C, $-CH_3$); EI-MS, m/z: 420.47(M^+, 29.3%); Anal. calcd. for ($C_{25}H_{20}N_6O$): C, 71.41; H, 4.79; N, 19.99%; Found: C, 71.43; H, 4.80; N, 19.97%.

2.4.9. (3-(Furan-2-yl)-4-methyl-6-phenyl pyrazolo[3,4-c] pyrazol-2(1*H*,3*H*,6*H*)-yl)(pyridin-4-yl)methanone (1i)

Light Yellow solid; Yield: 74%; (7.109mg); M.p. 166–168°C; IR(KBr) ν: 3323, 2974, 1655, 1640cm^{-1}; ^{1}H NMR(DMSO-d$_6$, 300 MHz): δ 8.36 (-Pyridin, d, *J* = 6.23 Hz, , 2H), 7.85 (s, 2H, -CH), 7.65 (1H, s, -CH), 7.58 (5H, -Ar ring, t, *J* = 6.21 Hz), 6.43 (1H, -CH, s), 6.23 (1H, s, -CH), 6.13 (CH, 1H, s), 4.0 (1H, s, -NH), 1.97 (s, -CH$_3$, 3H); ^{13}C NMR (DMSO-d$_6$, 75 MHz): δ 172.0 (1C, C=O), 149.0-106.7 (3C, -C), 152.5-106.7 (4C, -furan), 149.7-121.7 (5C, -pyridine), 139.7-123.9 (6C, -Ar ring), 67.1 (-CH, 1C), 12.7 (-CH$_3$, 1C); EI-MS, m/z: 371.39(M$^+$, 24.8%); Anal. calcd. for ($C_{21}H_{17}N_5O_2$): C, 67.91; H, 4.61; N, 18.86%; Found: C, 67.93; H, 4.63; N, 18.85%.

2.4.10. (4-methyl-6-phenyl-3-(pyridin-2-yl)pyrazolo[3,4-c]pyrazol-2(1*H*,3*H*,6*H*)-yl)(pyridin-4-yl)methanone (1j)

Yellow solid; Yield: 81%; (8.675mg); M.p. 157–159°C; IR(KBr) ν: 3323, 2974, 1655, 1640cm^{-1}; ^{1}H NMR(DMSO-d$_6$, 300 MHz): δ 8.36 (-Pyridin, d, *J* = 6.23 Hz, 2H), 7.42 (2H, -Pyridin, d, *J* = 6.22 Hz), 8.44 (s, 1H, -CH), 7.34 (3H, s, -CH), 7.58 (5H, t, *J* = 6.21 Hz, -Ar ring), 6.13 (1H, CH, s), 4.0 (1H, -NH, s), 1.93 (-CH$_3$, s, 3H); ^{13}C NMR (DMSO-d$_6$, 75 MHz): δ 172.0 (C=O, 1C), 145.8 (-CH, 3C), 158.7-120.7 (10C, -pyridine), 139.7-123.9 (6C, -Ar ring), 68.1 (-CH, 1C), 12.7 (1C, -CH$_3$); EI-MS, m/z: 382.42 (M$^+$, 24.0%); Anal. calcd. for ($C_{22}H_{18}N_6O$): C, 69.10; H, 4.74; N, 21.98%; Found: C, 69.12; H, 4.73; N, 21.97%.

2.4.11. (4-Methyl-6-phenyl-3-(thiazol-5-yl)pyrazolo[3,4-c]pyrazol-2(1*H*,3*H*,6*H*)-yl)(pyridin-4-yl)methanone (1k)

Light Yellow solid; Yield: 82%; (9.277mg); M.p. 150–153°C; IR(KBr) ν: 3323, 2974, 1655, 1640cm^{-1}; ^{1}H NMR(DMSO-d$_6$, 300 MHz): δ 8.36 (-Pyridin, 2H, d, *J* = 6.23 Hz), 8.82 (1H, s, -CH), 7.85 (2H, d, *J* = 6.22 Hz, -Pyridin), 7.58 (5H, -Ar ring, t, *J* = 6.21 Hz), 7.16 (1H, s, -CH), 6.13 (s, 1H,-CH), 4.0 (1H, s, -NH), 1.97 (3H, -CH$_3$, s); ^{13}C NMR (DMSO-d$_6$, 75 MHz): δ 172.0 (1C, C=O), 145.8 (3C, -C), 153.7 (1C, -CH), 141.8 (1C, -CH), 149.7-121.7 (5C, -pyridine), 139.7-123.4 (6C, -Ar ring), 133.3 (1C, -CH), 66.1 (1C, -CH), 12.6 (1C, -CH$_3$); EI-MS, m/z: 388.45 (M$^+$, 24.7%); Anal. calcd.

for ($C_{20}H_{16}N_6OS$): C, 61.82; H, 4.15; N, 21.63; S, 8.25%; Found: C, 61.83; H, 4.14; N, 21.61; S, 8.24%.

2.4.12.(3-(Benzo[d][1,3]dioxol-5-yl)-4-methyl-6-phenylpyrazolo[3,4-c]pyrazol-2(1*H*,3*H*,6*H*)-yl)(pyridin-4-yl)methanone (1l)

Yellow solid; Yield: 83% (11.382mg); M.p. 171–172°C; IR(KBr) ν: 3323, 2974, 1655, 1640cm^{-1}; ^{1}H NMR(DMSO-d_6, 300 MHz): δ : δ 8.36 (-Pyridin, 2H, d, *J* = 6.23 Hz), 7.42 (2H, -Pyridin, d, *J* = 6.22 Hz), 6.73 (dd, *J* = 7.33 Hz, *J* = 7.37 Hz, 3H, -Ar ring), 7.58 (5H, t, *J* = 6.21 Hz, -Ar ring), 6.16 (s, -CH, 1H), 6.03 (2H, s, -CH_2), 4.0 (1H, -NH, s), 1.97 (s, 3H, -CH_3); ^{13}C NMR (DMSO-d_6, 75MHz): δ 172.0 (C=O, 1C), 145.8 (3C, -C), 149.7-121.7 (5C, -pyridine), 148.6-112.0 (12C, -Ar ring), 101.2 (1C, -CH_2), 68.4 (-CH, 1C), 12.7 (1C, -CH_3); EI-MS, m/z: 425.44 (M^+, 27.9%); Anal. calcd. for ($C_{24}H_{19}N_5O_3$): C, 67.72; H, 4.50; N, 16.46%; Found: C, 67.75; H, 4.52; N, 16.44%.

Biological activity

Antibacterial activity

Additionally, six species of clinical bacterial isolates and two species of yeast cells were obtained from various clinical laboratories. To prepare fresh overnight bacterial cultures, a loop was used to transfer inoculate from stock cultures to test tubes containing nutrient broth that had been sterilized at 121°C for 20 minutes. All bacterial strains were maintained on nutrient agar slants (Hi-Media) at 37°C ± 0.1°C. Candida spp. was propagated on Sabouraud Dextrose agar slants (Hi-Media).

Cytotoxic activity

The synthesized compounds were screened for cytotoxicity activity against MCF-7 cell line and normal Vero cell line cell lines. All compounds (**1a-l**) was significantly low active compared with other compounds and standard doxorubicin (LC_{50} = 21.05 ± 0.82 μg/mL). As a result, both cell lines were exposed to cytotoxicity of compound **1c**, which was found to be extremely active against antioxidant activities.

Three cell lines were treated with these compounds at one primary cytotoxic assay dose of 100μM for 48 h (MTT anticancer assay). Doxorubicin was used as a standard.

In the current protocol, all cell lines were pre-incubated on a microtiter plate. The results of each test were reported as the growth percentage of treated cells compared to untreated control cells.

Compounds reducing the growth of any one of the cell lines to approximately 32% or less were described as having cytotoxic activity. A 0.1mL aliquot of the cell suspension (5×10^6 cells/100 µL) and 0.1 mL of the test solution (6.25–100 µg in 1% DMSO, with the final DMSO concentration in media less than 1%) were added to the wells, with the plates kept in an incubator (5% CO_2) at 37 °C for 72 h. The blank sample contained only the cell suspension, and the control wells contained 1% DMSO and the cell suspension. After 72 h, 20 µL of MTT was added, and the plates were kept in the CO_2 incubator for 2 h, followed by the addition of propanol (100 µL). The plates were covered with aluminum foil to protect them from light and subsequently agitated in a rotary shaker for 10–20 min. Afterwards, the 27-well plates were processed on an ELISA reader to obtain absorption data at 562 nm.

Molecular dynamics simulations

Molecular dynamics simulation was carried out using Desmond and Schrödinger software to explore the stability of ligand **1b** and **1g** docked complexes with proteins 1AI9 and 1AJ0. The ligand topology was generated by the PRODRG server and combined with the protein topology using the GROMOS 43a1 force field and a solvation method involving a single point charge (SPC) water model. The system was framed with a cubic box at a distance of 2 nm from the box to the protein surface. The necessary ions were added to neutralise the system, and the docked complex energy was minimised using the steepest descent algorithm. The LINCS algorithm was used to constrain the bond lengths and electrostatics computed using the PME method. The NVT and NPT ensembles were used to equilibrate the systems for each 100 ps, with a reference temperature of 300 K, using the V-rescale thermostat. The production MD run was conducted for 10 ns with a time step of 2 fs, and the docked complex structure coordinates were saved every 10 ps for further analysis. The results were analysed using RMSD, RMSF, gyration, and hydrogen bond plots, and Xmgrace software was used to plot the graphs.

RMSD analysis

The Root Mean Square Deviation (RMSD) values indicate the stability of complex structures. Analysing the RMSD plot of complex 1AI9 with **1b**, it was observed that the complex was stable between 20 and 40 ns and 40–50 ns, as the peak fluctuation of the Cα backbone of the protein and heavy atoms of the ligand were within the range shown in Fig. 9(a). On the other hand, analysis of the complex structure of 1AJ0 with **1g** revealed that the Cα backbone atoms and heavy atoms of the ligand fluctuated, as shown in Fig. 9(b), which indicates that the complex was not stable. Therefore, RMSD study of both complexes, 1AI9 with **1b** and 1AJ0 with **1g**, provided insights into their stability.

RMSF analysis

Root Mean Square Fluctuation (RMSF) analysis was used to evaluate changes in the protein chain during the simulation. No fluctuations were observed in the amino acid residues, except for the N- and C-terminal residues. All residues were within an unacceptable range (Fig. 10(a–b)).

Based on this MD simulation analysis, compound ligands 1b and 1g were stable and exhibited good interactions with important protein residues (Fig. 11(a–b)–12(a–b)). Therefore, these compounds may be effective inhibitors of the 1AI9 and 1AJ0 proteins.

^{1}H NMR and ^{13}C NMR spectrum of compounds (1a-1l)

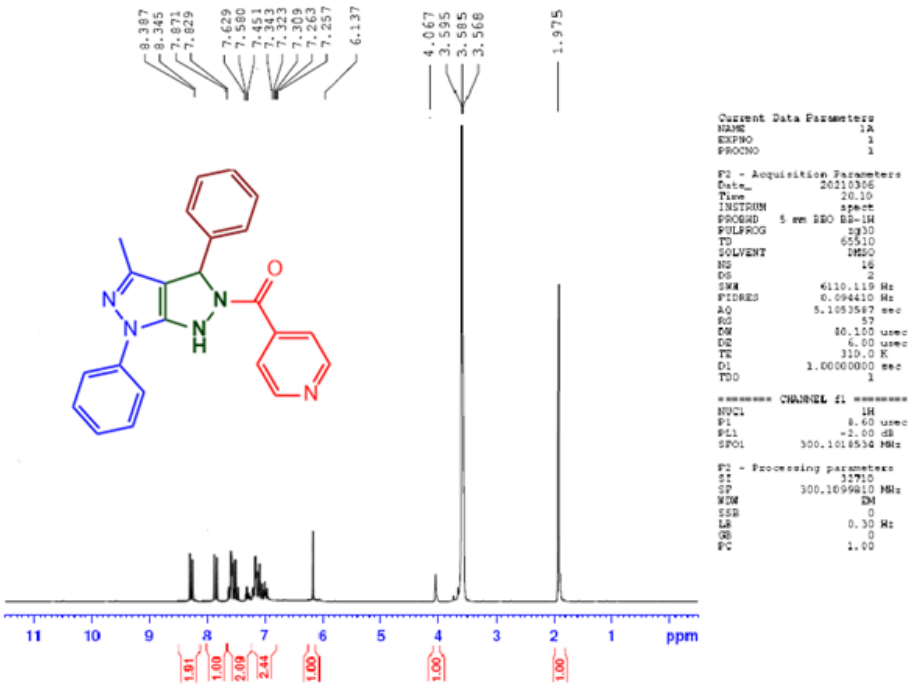

Figure S1. ^{1}H NMR spectrum of the compound **1a**

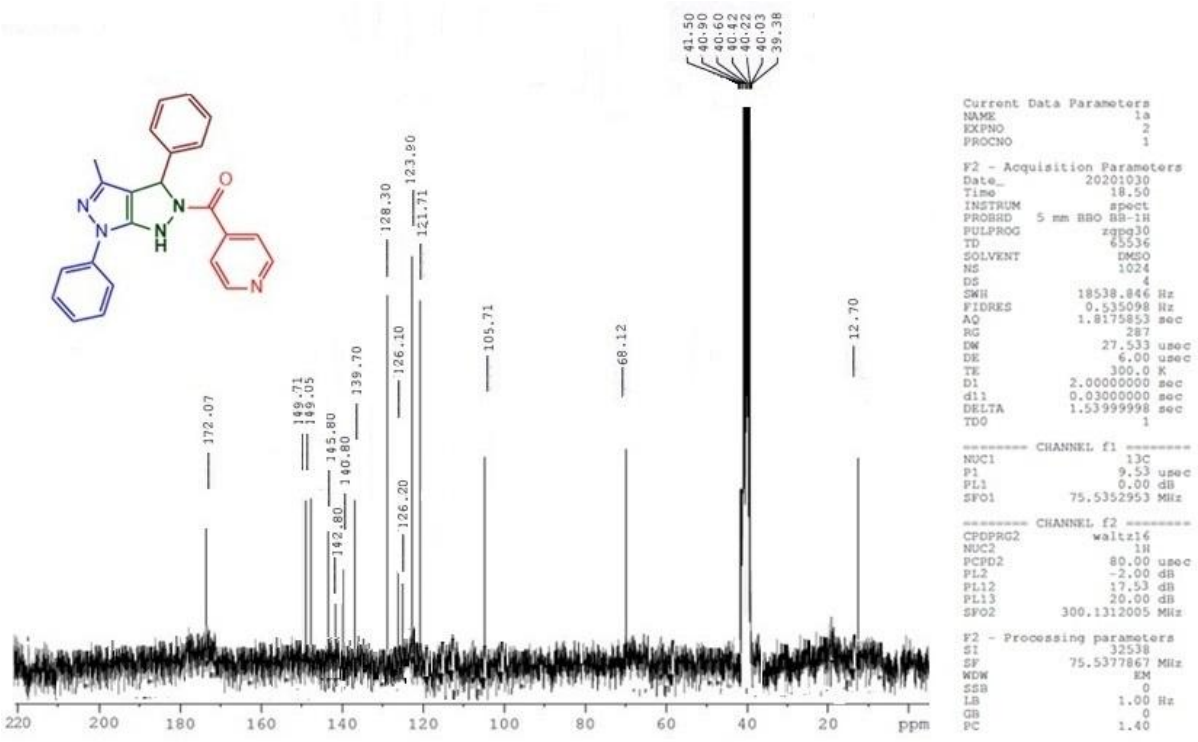

Figure S2. ^{13}C NMR spectrum of the compound **1a**

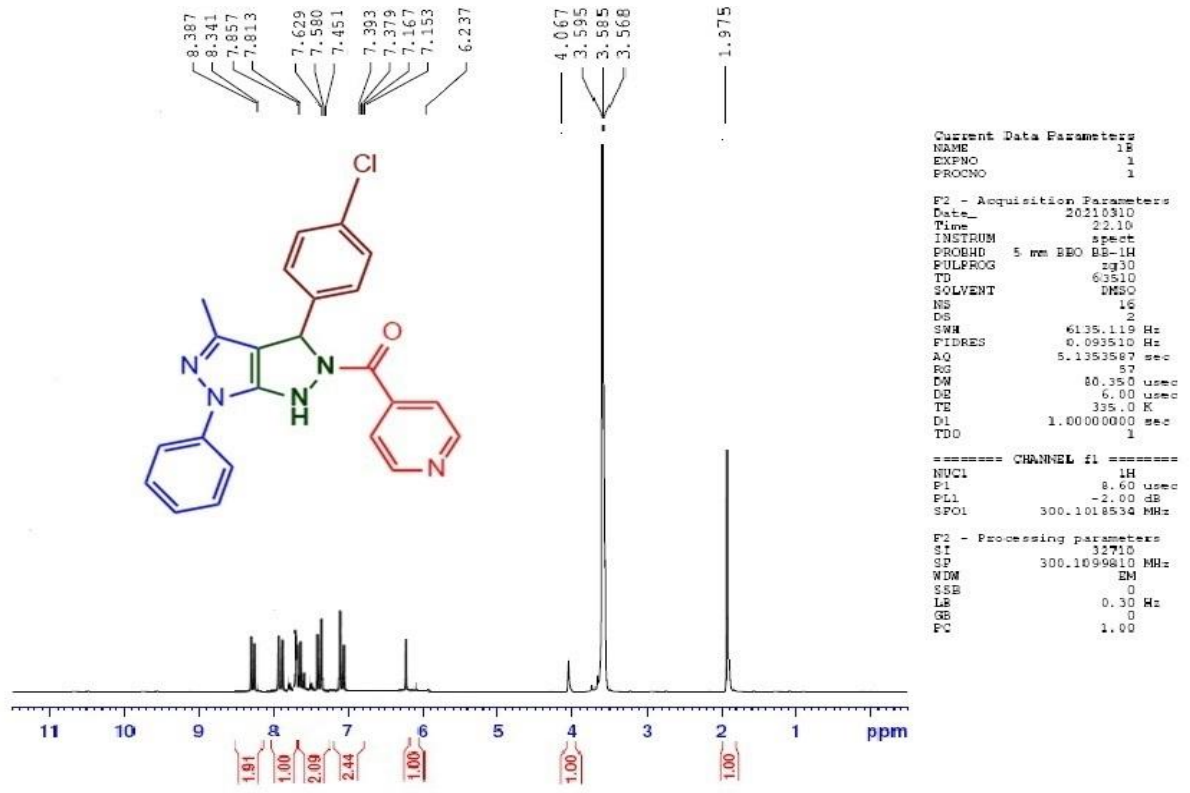

Figure S3. ^{1}H NMR spectrum of the compound **1b**

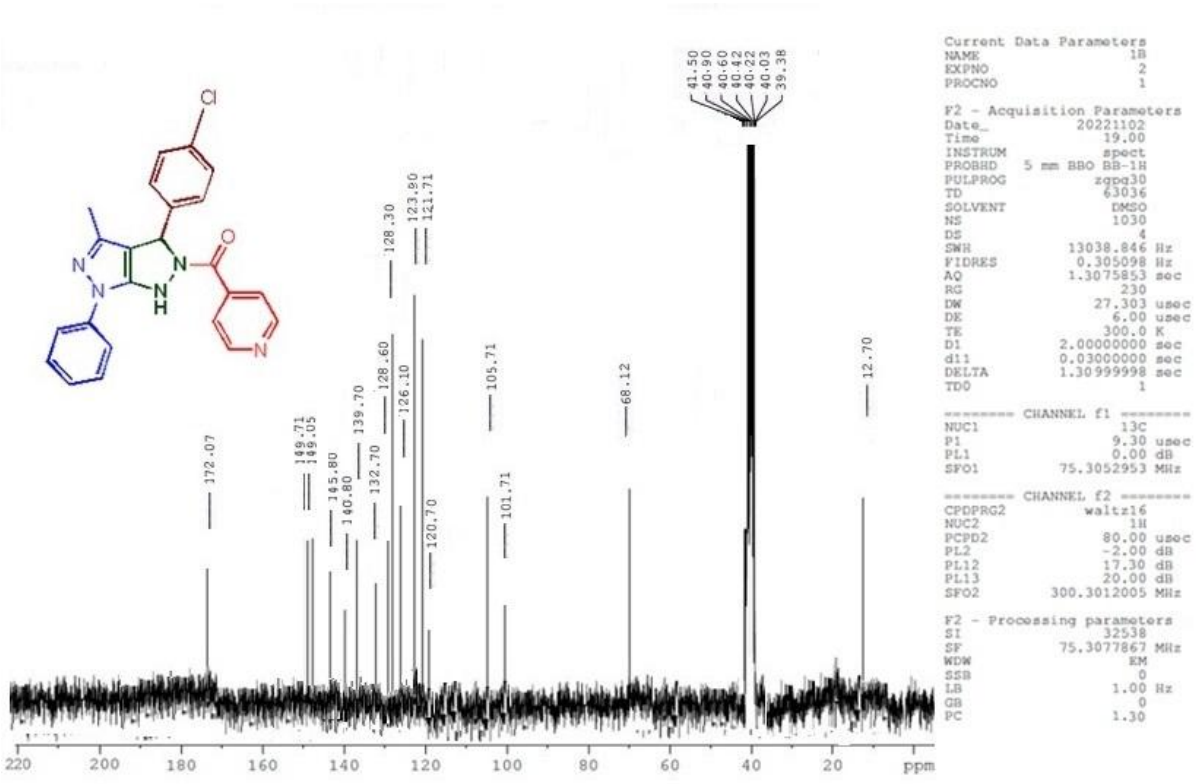

Figure S 4. ^{13}C NMR spectrum of the compound **1b**

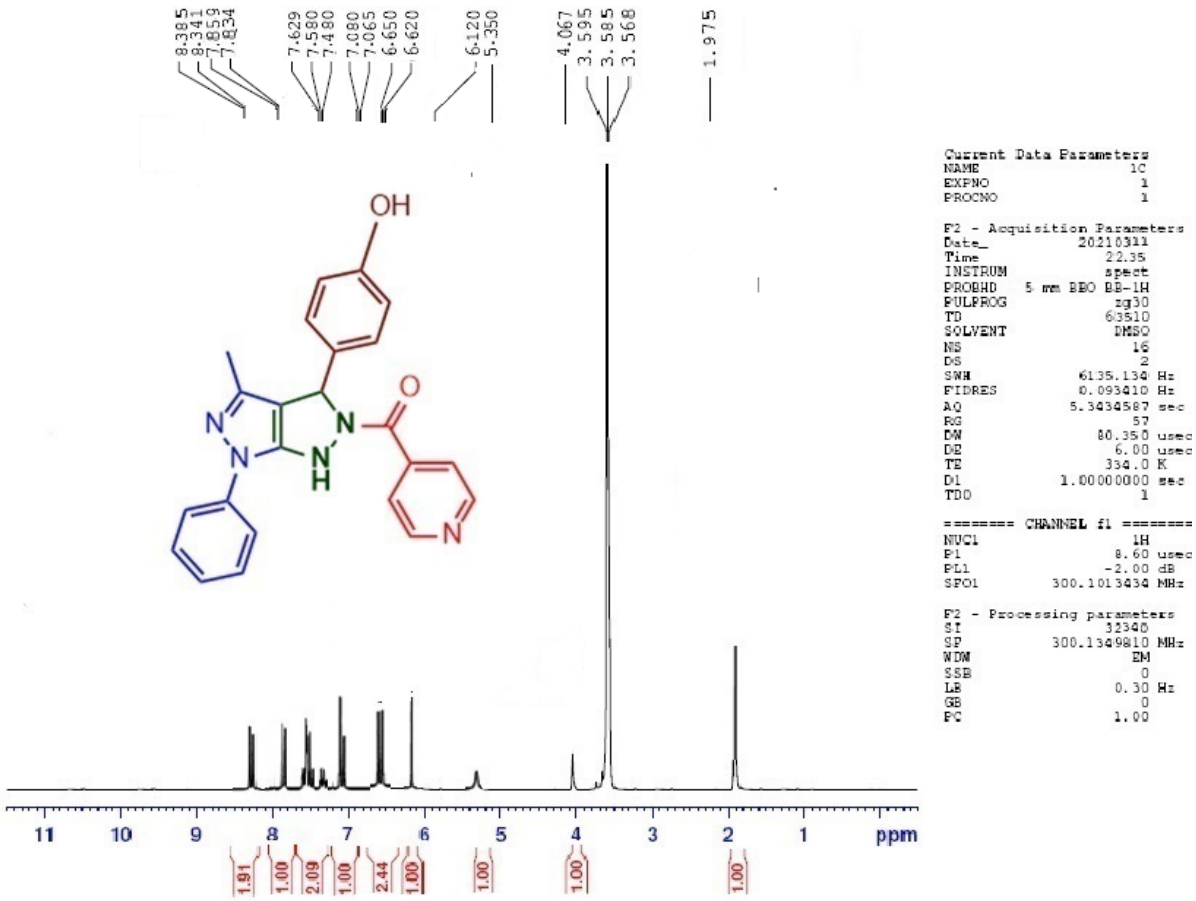

Figure S5. ^{1}H NMR spectrum of the compound **1c**

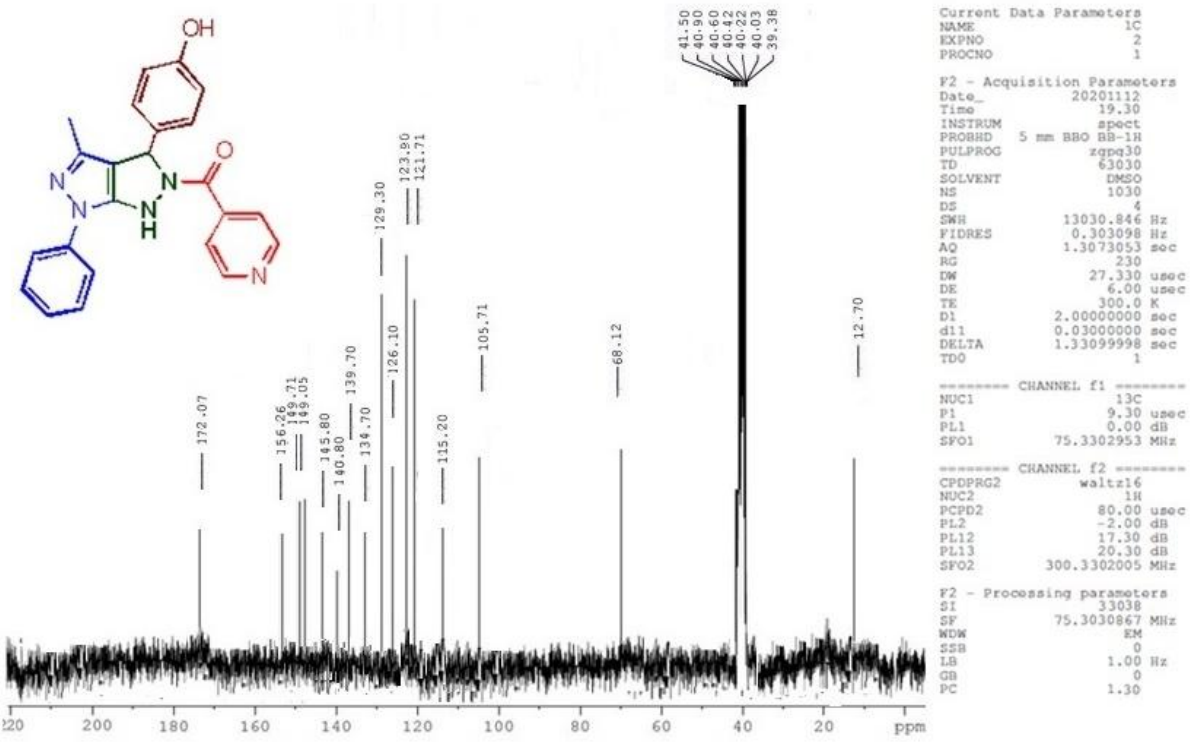

Figure S6. ^{13}C NMR spectrum of the compound **1c**

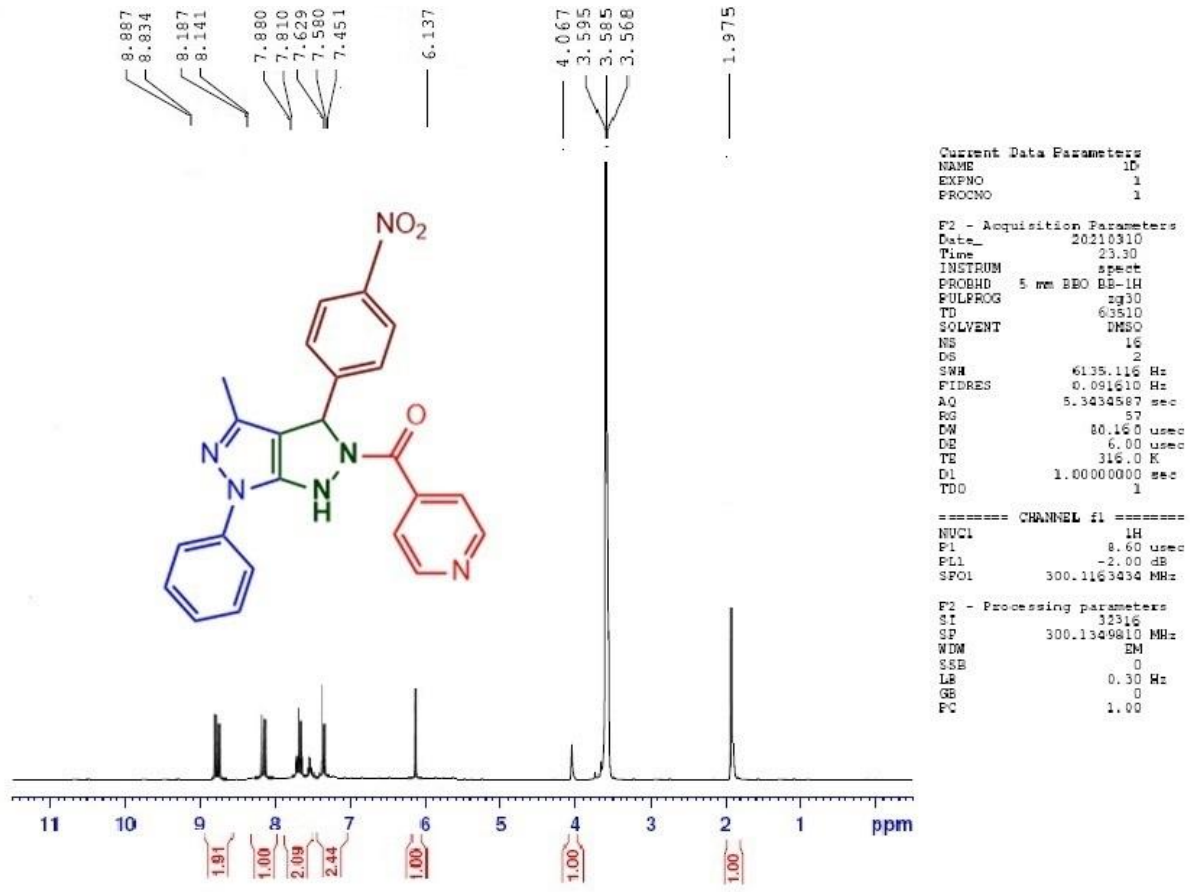

Figure S7. ^{1}H NMR spectrum of the compound **1d**

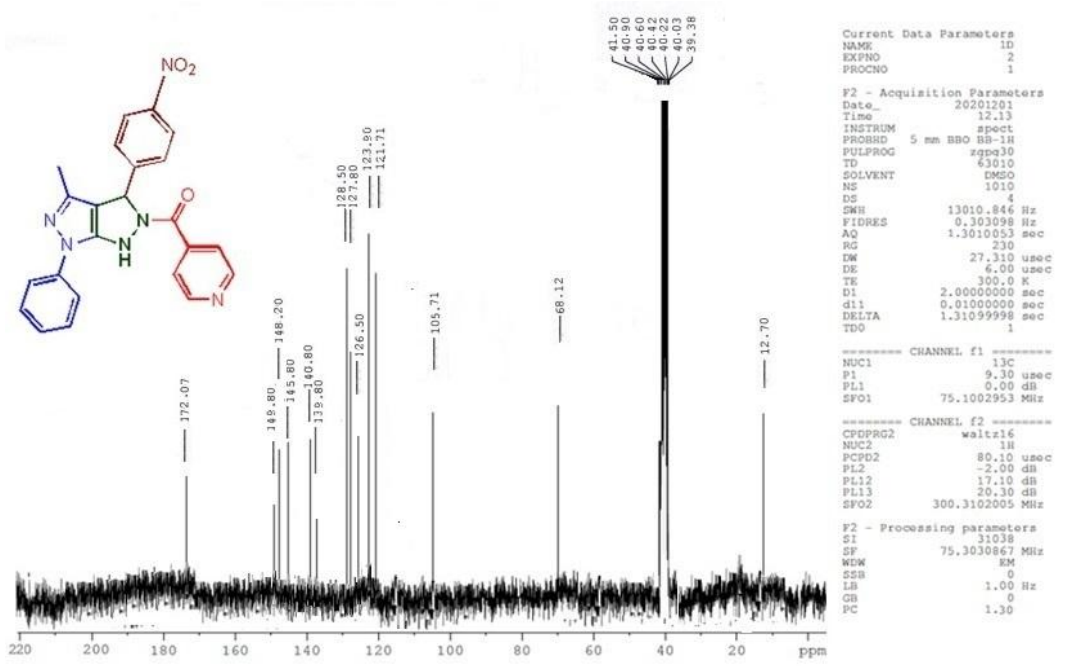

Figure S8. ^{13}C NMR spectrum of the compound **1d**

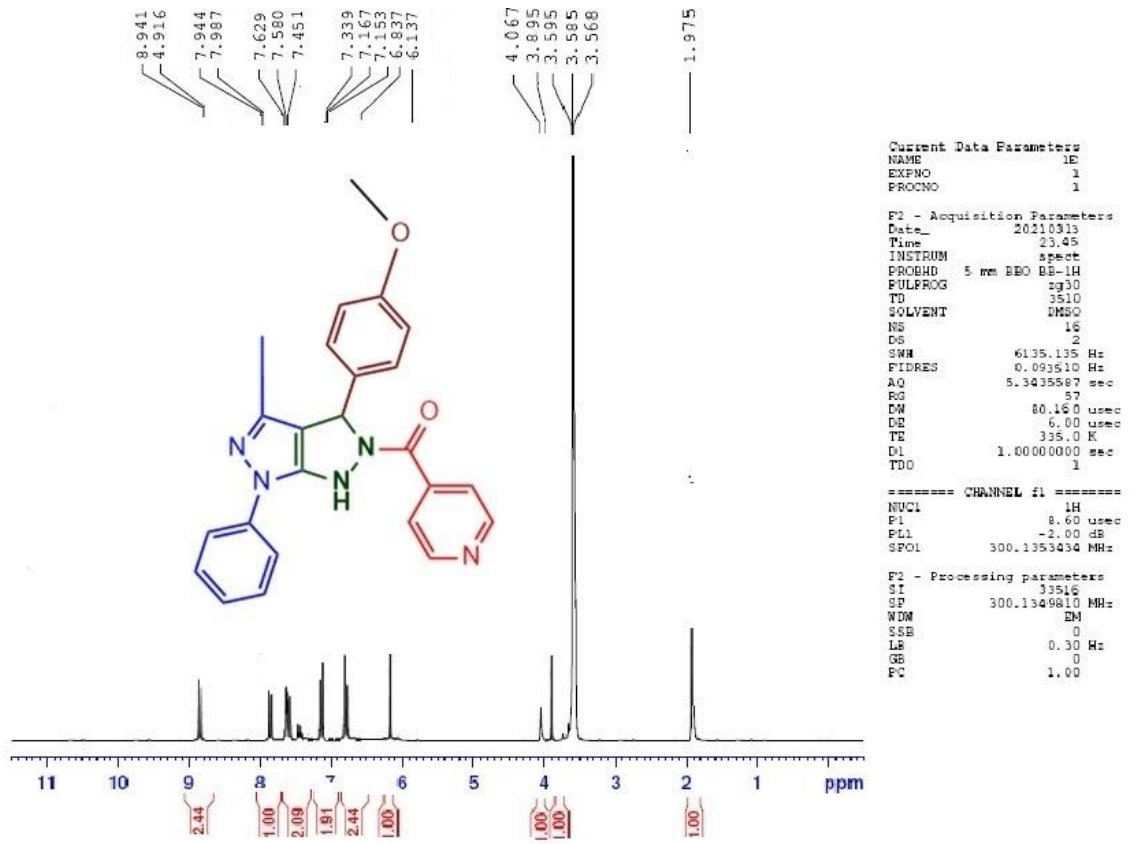

Figure S9. ^{1}H NMR spectrum of the compound **1e**

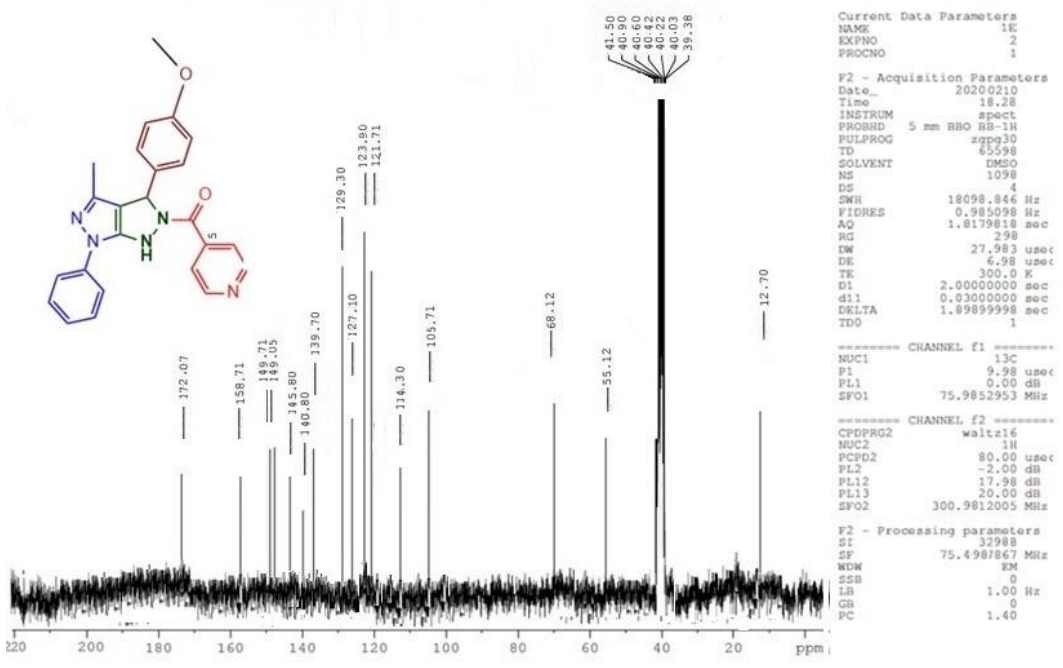

Figure S10. ^{13}C NMR spectrum of the compound **1e**

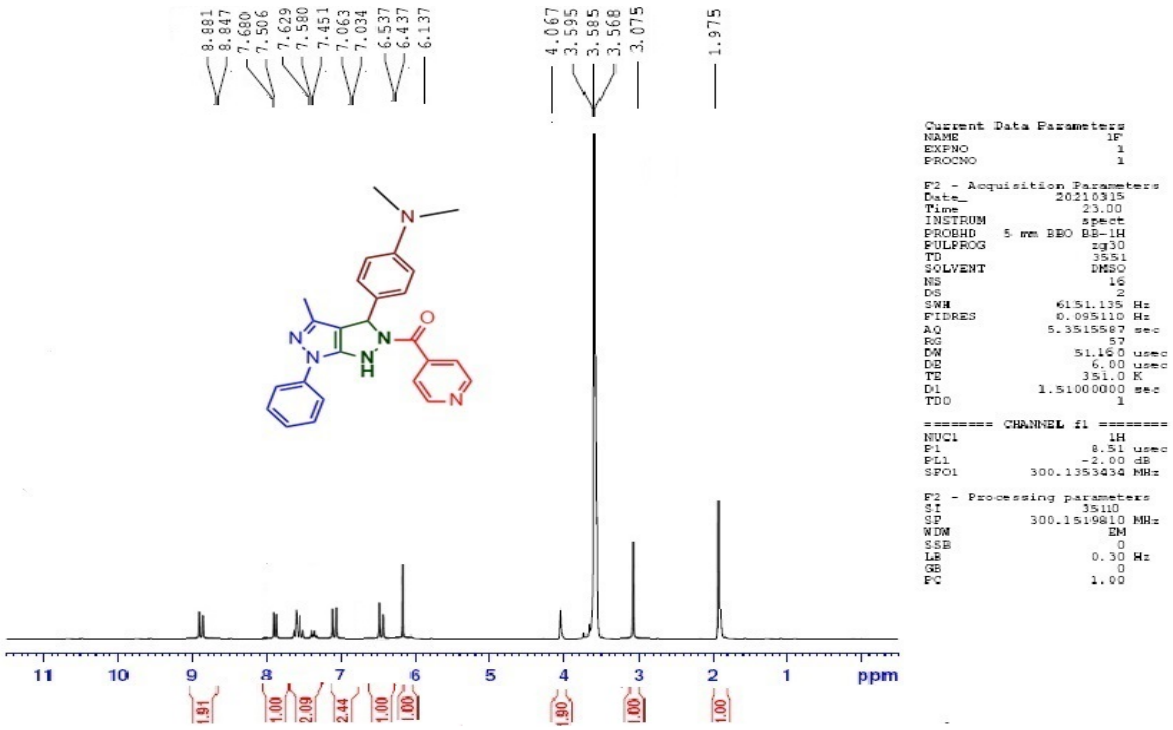

Figure S11. ^{1}H NMR spectrum of the compound **1f**

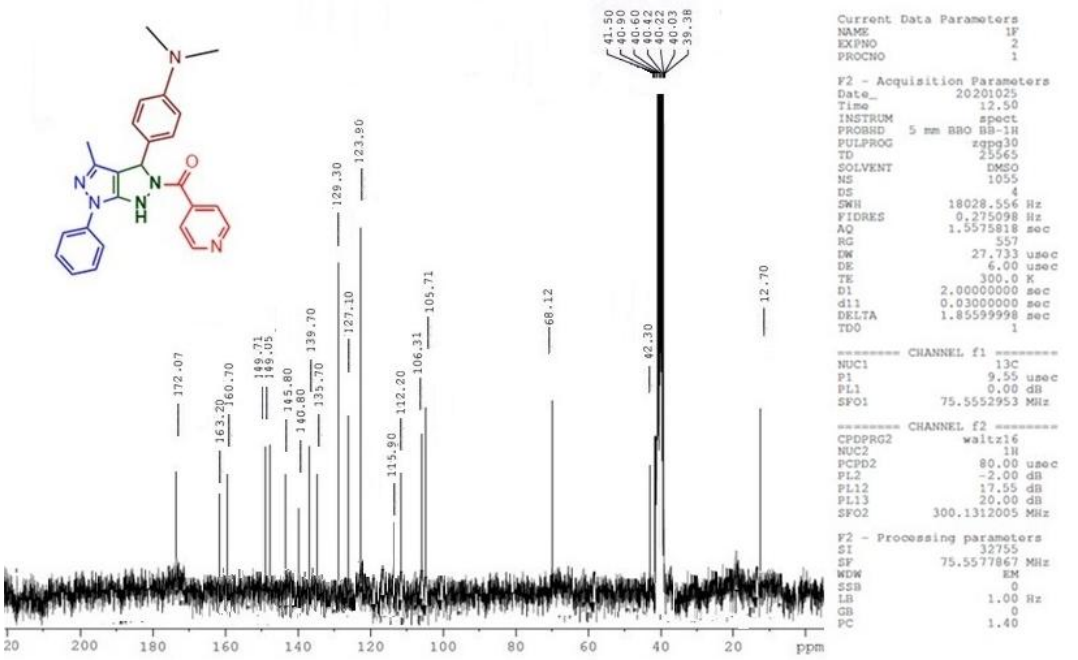

Figure S12. ^{13}C NMR spectrum of the compound **1f**

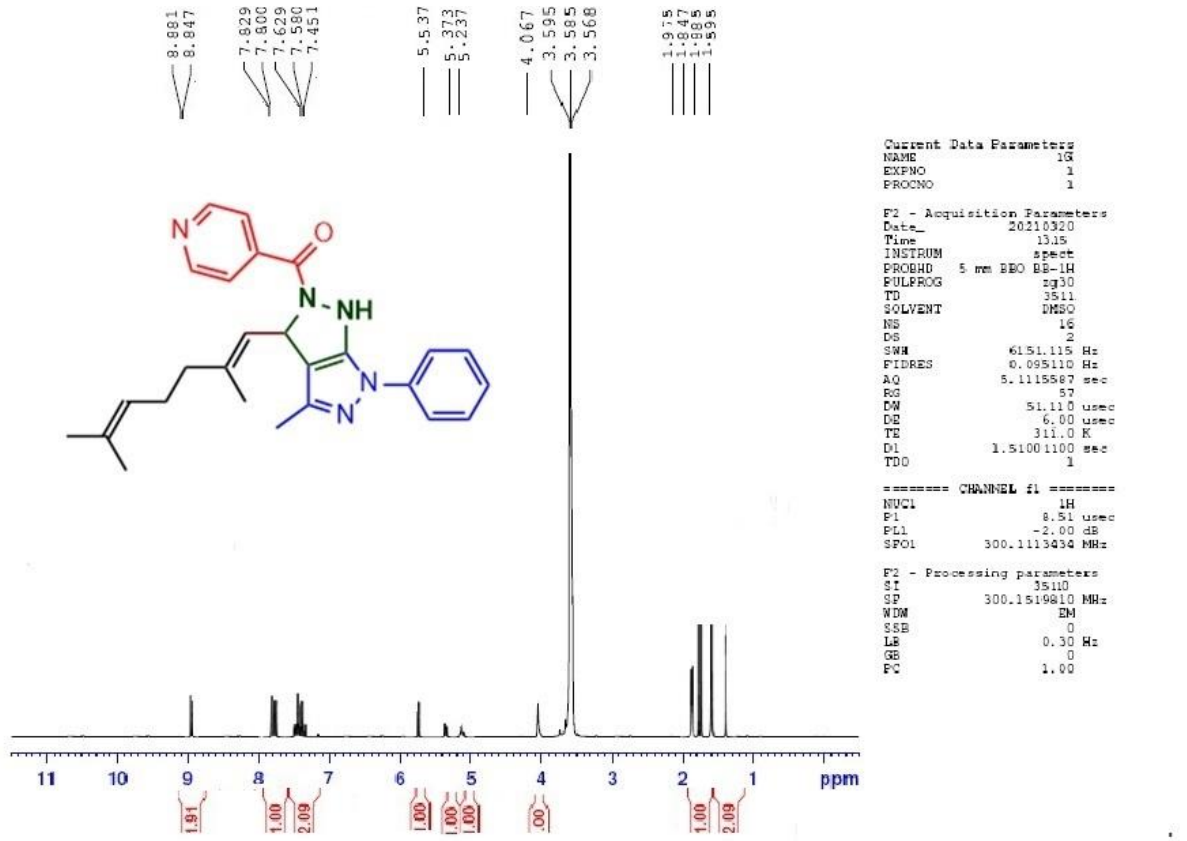

Figure S13. ^{1}H NMR spectrum of the compound **1g**

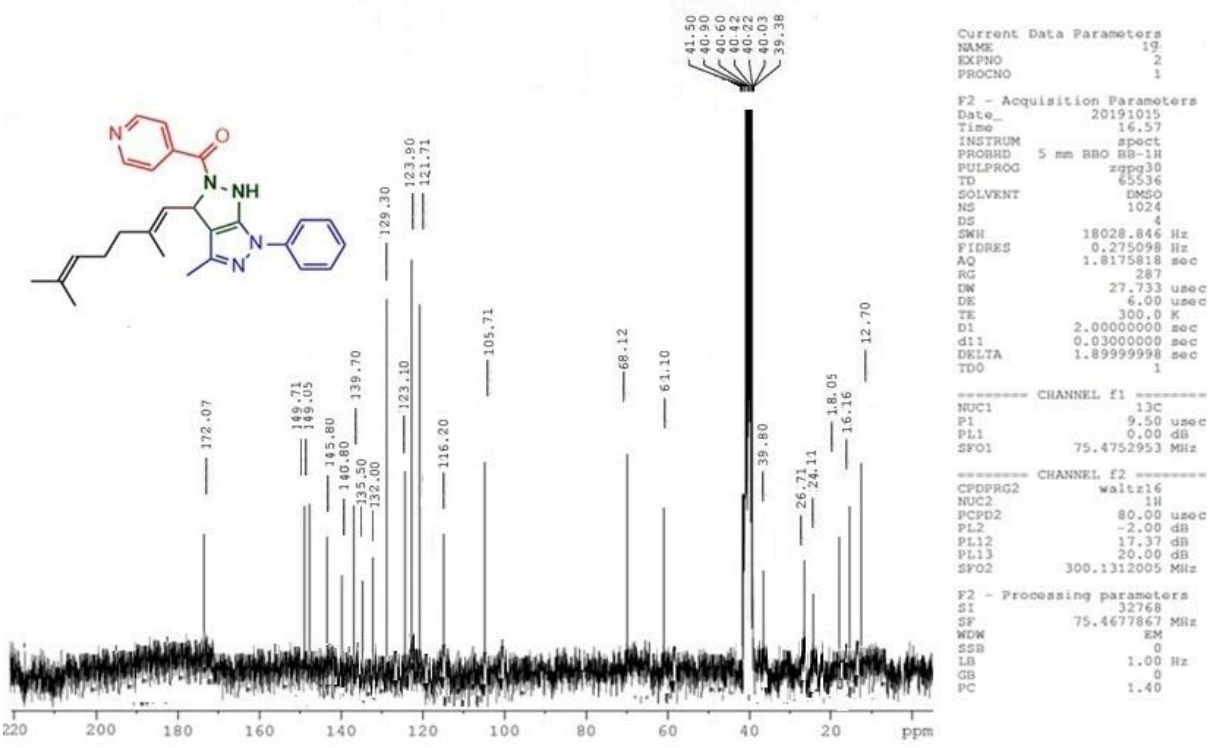

Figure S14. ^{13}C NMR spectrum of the compound **1g**

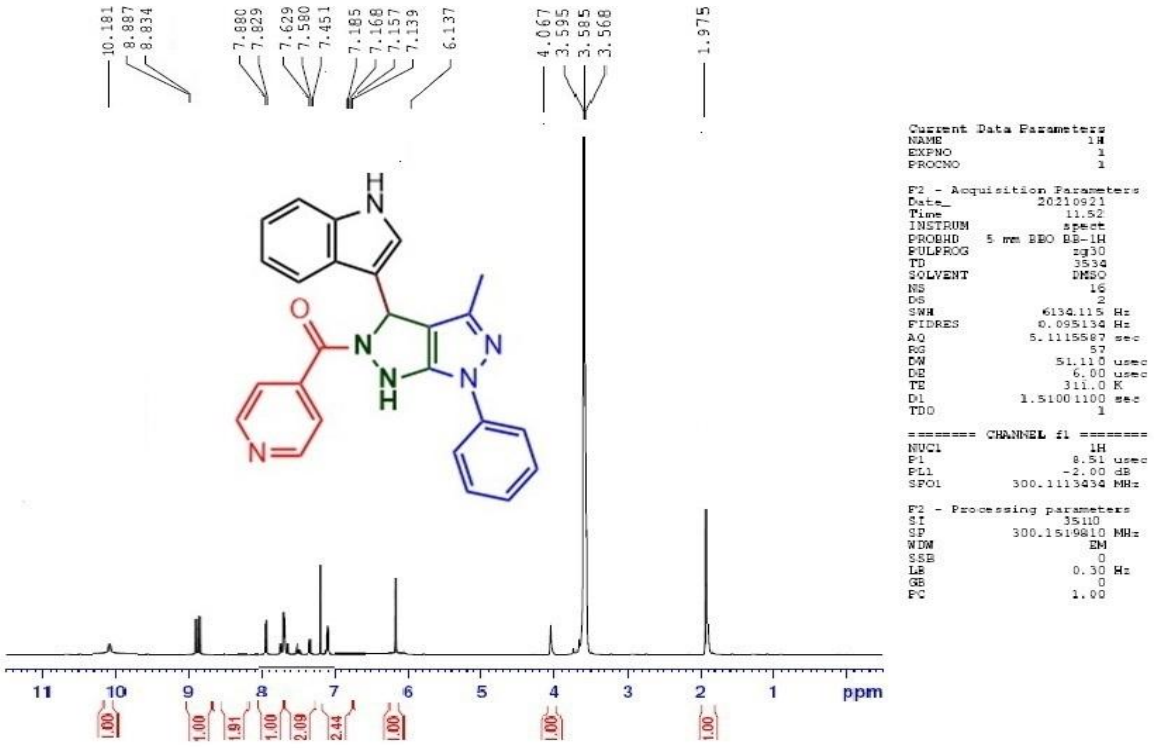

Figure S15. ^{1}H NMR spectrum of the compound **1h**

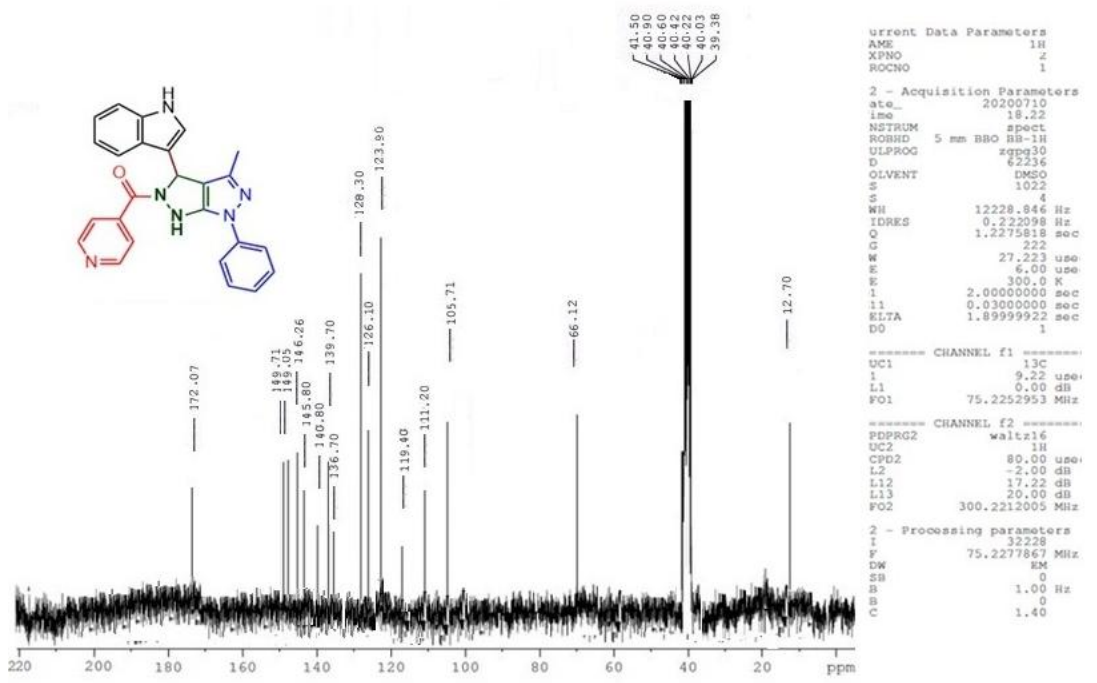

Figure S16. ^{13}C NMR spectrum of the compound **1h**

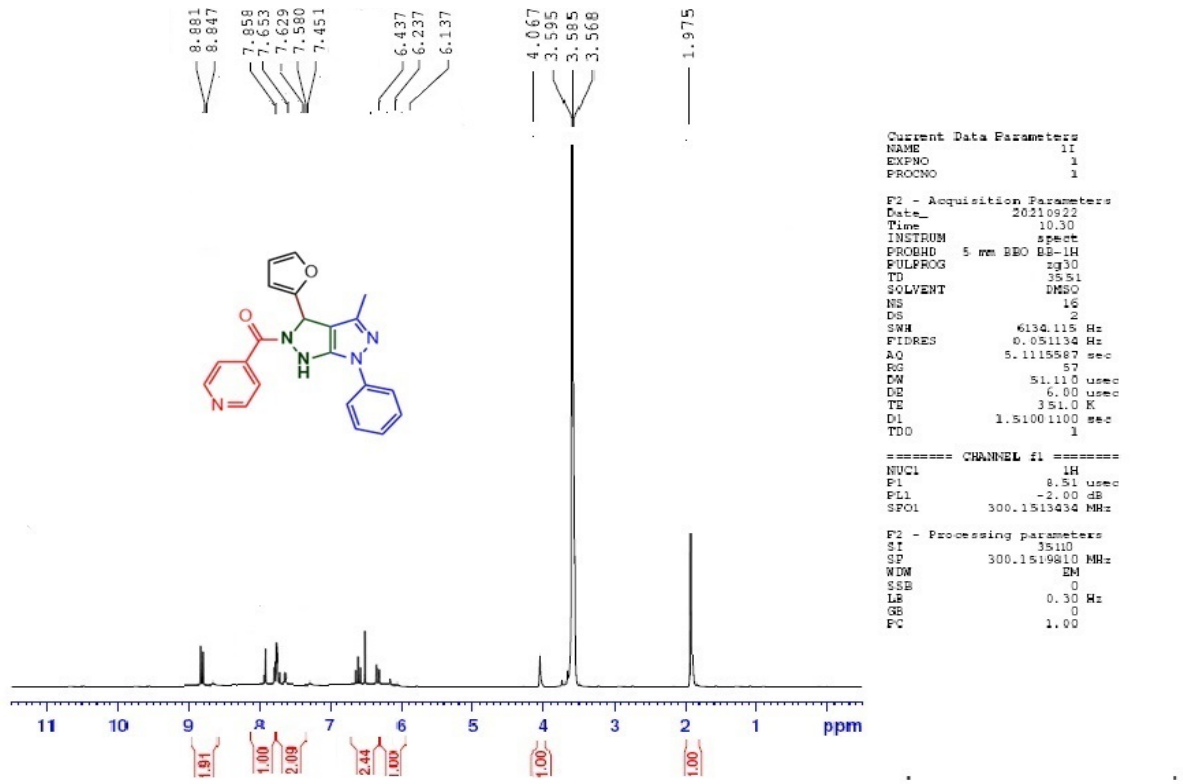

Figure S17. ^{1}H NMR spectrum of the compound **1i**

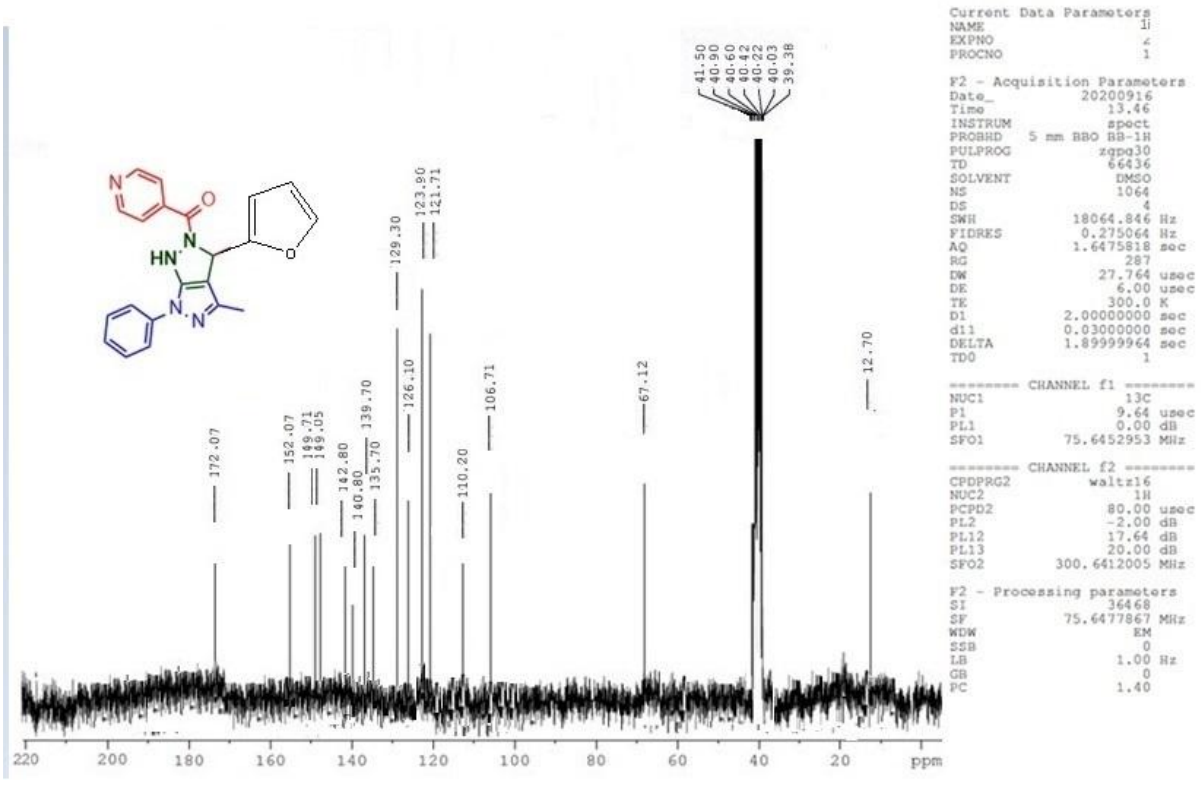

Figure S18. ^{13}C NMR spectrum of the compound **1i**

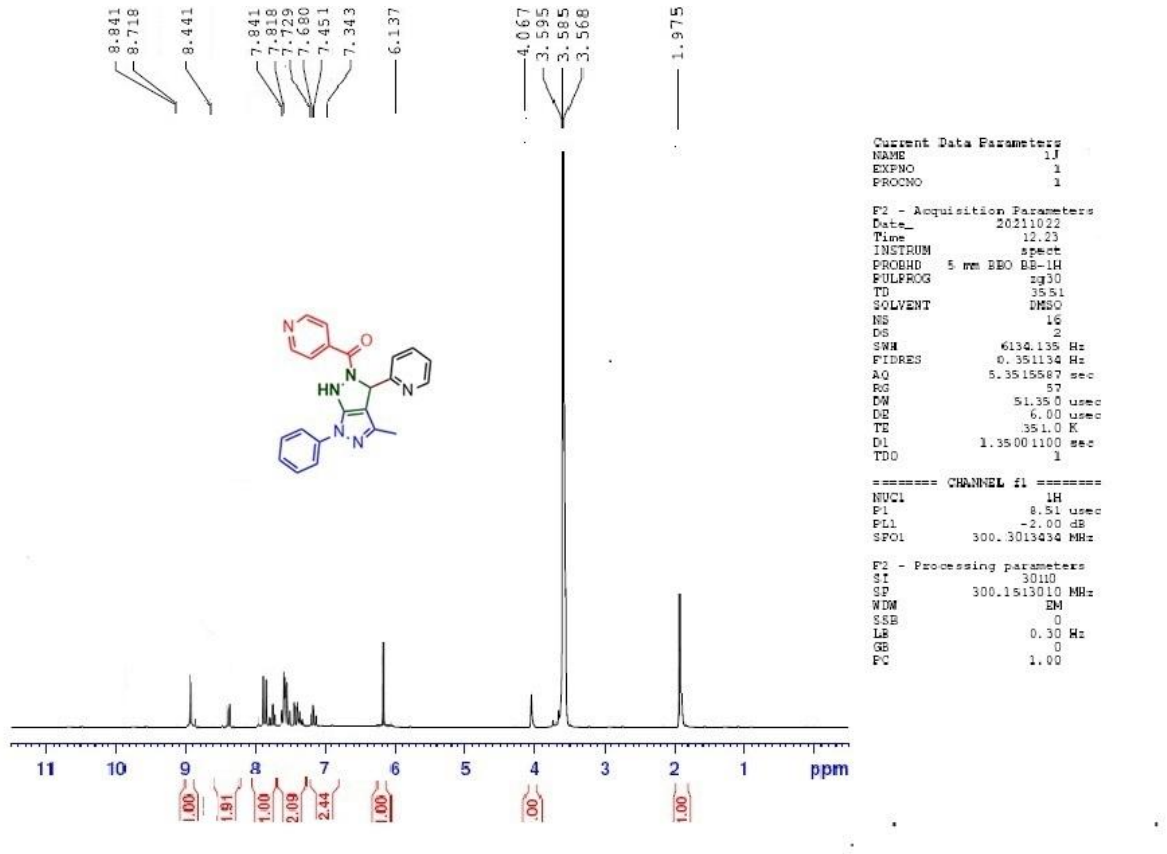

Figure S19. ^{1}H NMR spectrum of the compound **1j**

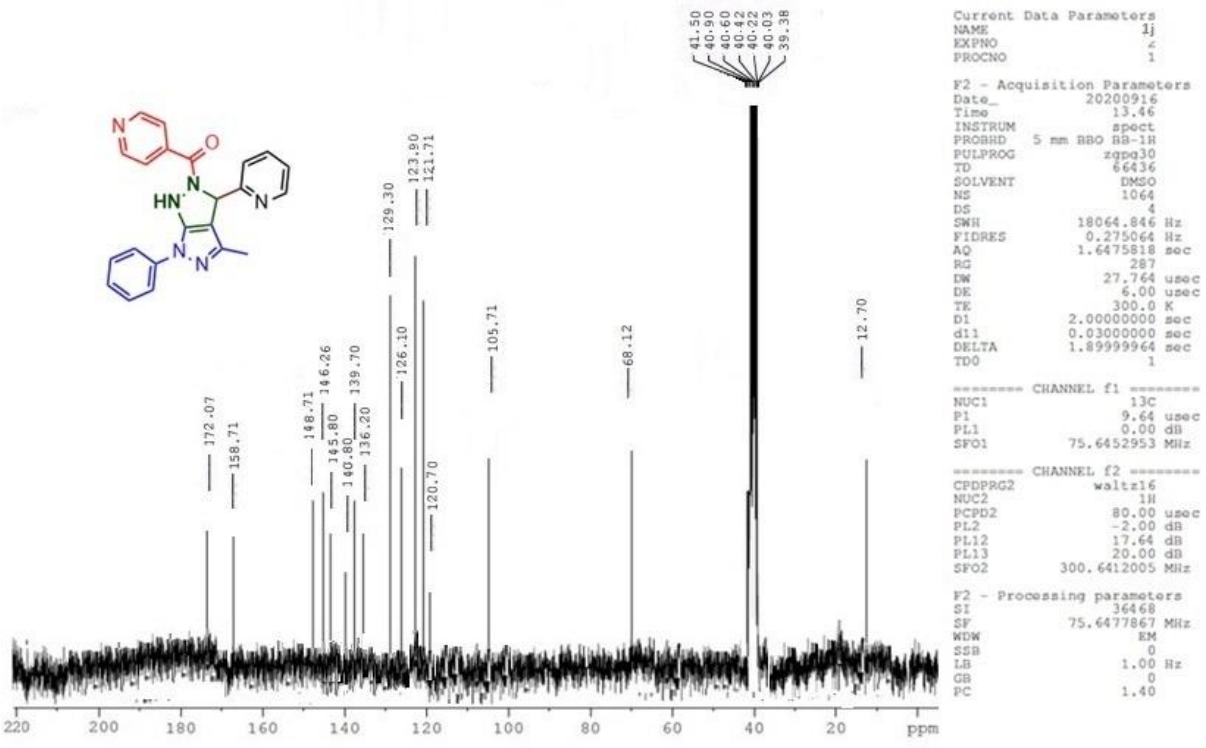

Figure S20. ^{13}C NMR spectrum of the compound **1j**

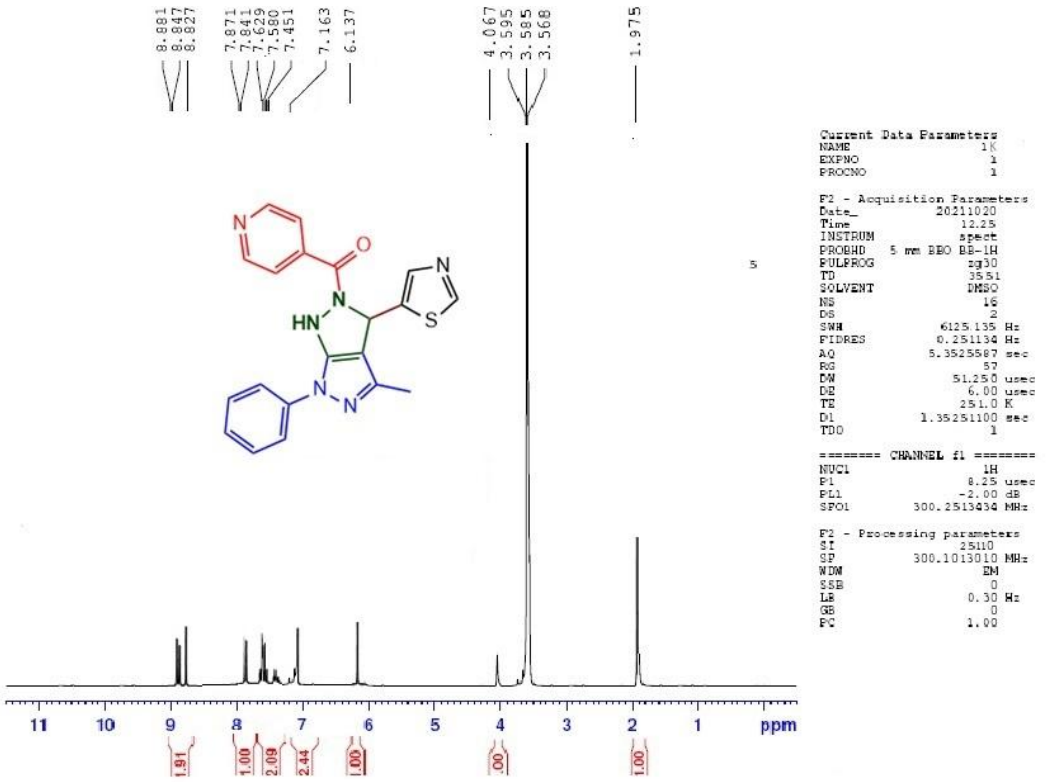

Figure S21. ^{1}H NMR spectrum of the compound **1k**

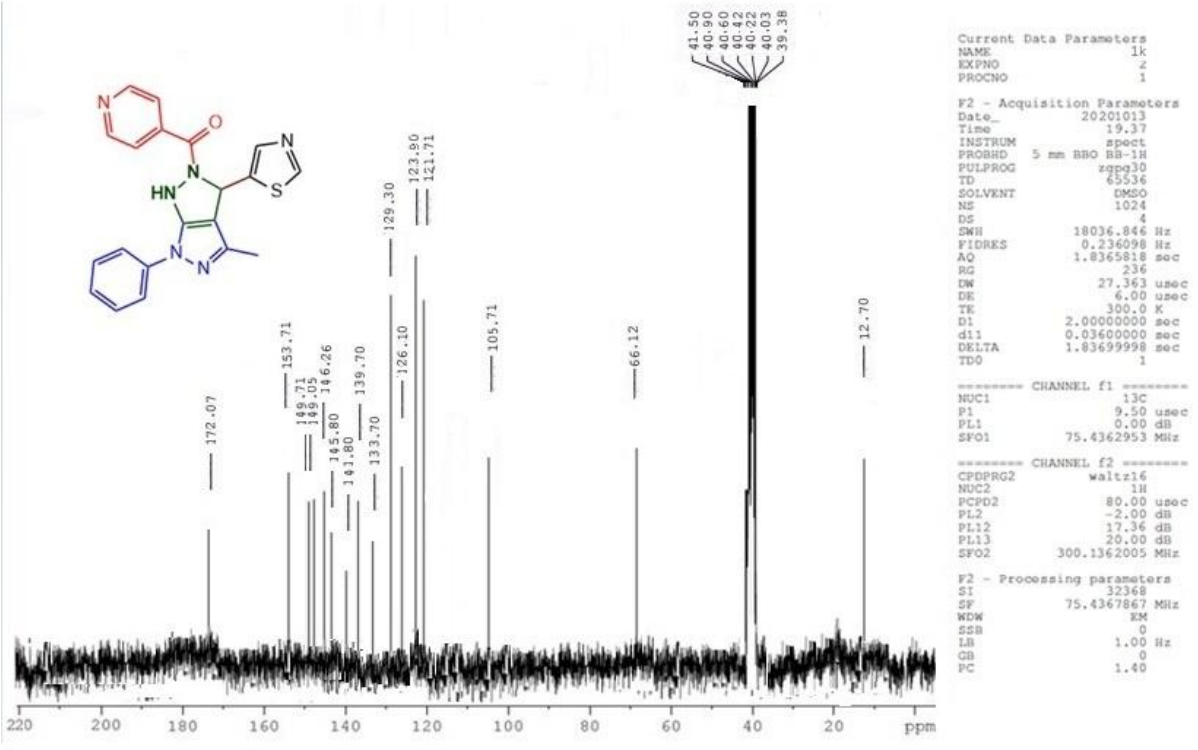

Figure S22. ^{13}C NMR spectrum of the compound **1k**

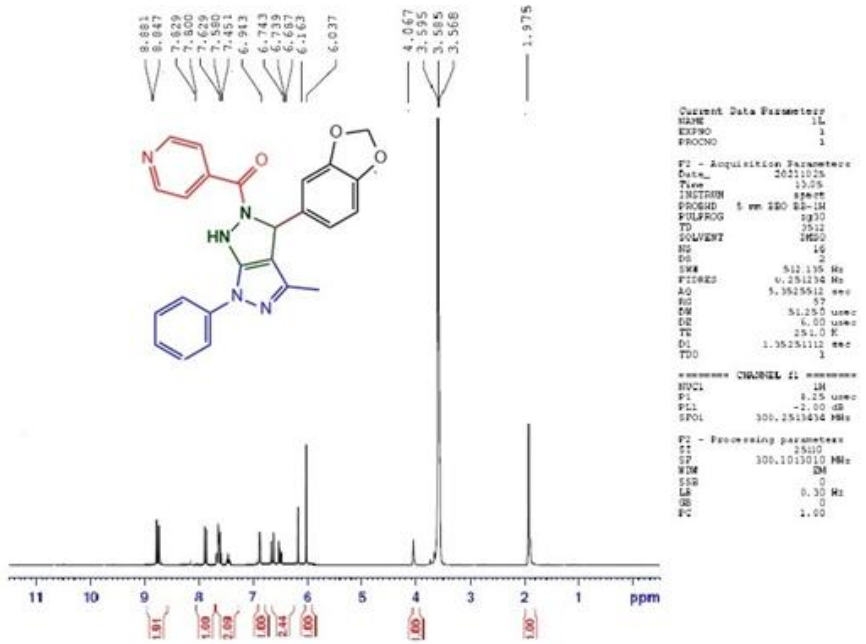

Figure S23. ^{1}H NMR spectrum of the compound **1l**

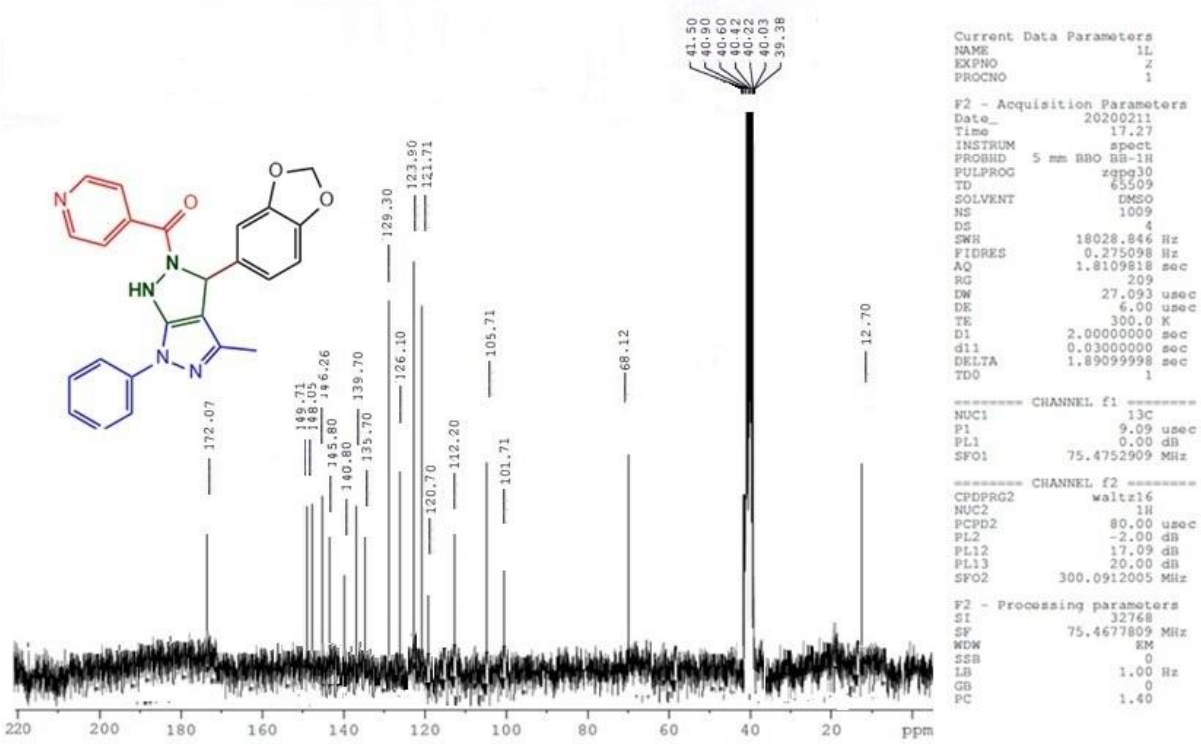

Figure S24. ^{13}C NMR spectrum of the compound **1l**

Molecular dynamics simulations for compound 1b

SCHRÖDINGER.

Simulation Interactions Diagram Report

Simulation Details

Jobname: **desmond_md_job_1**
Entry title: **Full System**

CPU #	Job Type	Ensemble	Temp. [K]	Sim. Time [ns]	# Atoms	# Waters	Charge
1	mdsim	NPT	300.0	50.096	16203	4727	0

Protein Information

Tot. Residues	Prot. Chain(s)	Res. in Chain(s)	# Atoms	# Heavy Atoms	Charge
111	'A'	111	1942	924	+6

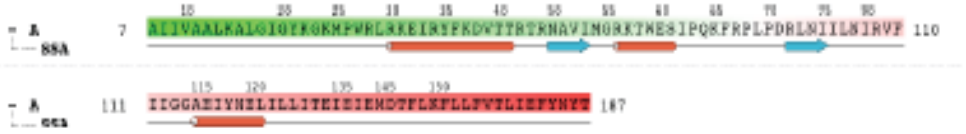

Ligand Information

SMILES	c1cc(Cl)ccc1[C@@H]2N(C(=O)c3ccncc3)Nc(c24)n(nc4C)-c5ccccc5
PDB Name	'UNK'
Num. of Atoms	48 (total) 30 (heavy)
Atomic Mass	415.886 au
Charge	0
Mol. Formula	C23H18ClN5O
Num. of Fragments	2
Num. of Rot. Bonds	4

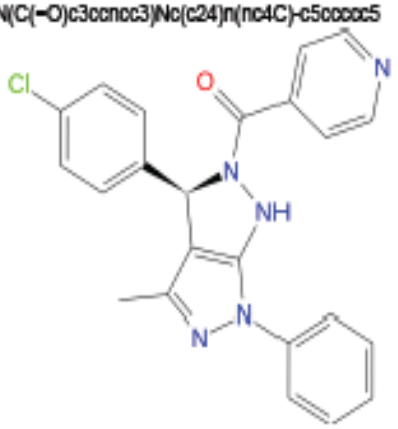

Counter Ion/Salt Information

Type	Num.	Concentration [mM]	Total Charge
Cl	19	73.081	-19
Na	13	50.003	+13

Protein-Ligand RMSD

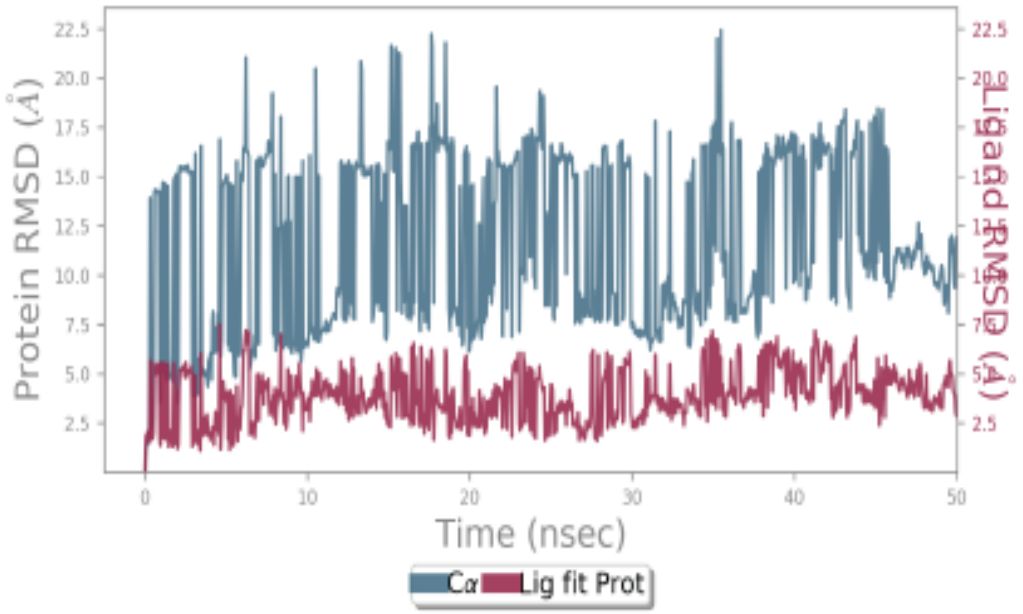

The Root Mean Square Deviation (RMSD) is used to measure the average change in displacement of a selection of atoms for a particular frame with respect to a reference frame. It is calculated for all frames in the trajectory. The RMSD for frame *x* is:

$$RMSD_x = \sqrt{\frac{1}{N}\sum_{i=1}^{N}(r'_i(t_i) - r_i(t_{ref}))^2}$$

where *N* is the number of atoms in the atom selection; t_{ref} is the reference time, (typically the first frame is used as the reference and it is regarded as time *t*=0); and *r'* is the position of the selected atoms in frame *x* after superimposing on the reference frame, where frame *x* is recorded at time t_x. The procedure is repeated for every frame in the simulation trajectory.

Protein RMSD: The above plot shows the RMSD evolution of a protein (left Y-axis). All protein frames are first aligned on the reference frame backbone, and then the RMSD is calculated based on the atom selection. Monitoring the RMSD of the protein can give insights into its structural conformation throughout the simulation. RMSD analysis can indicate if the simulation has equilibrated — its fluctuations towards the end of the simulation are around some thermal average structure. Changes of the order of 1-3 Å are perfectly acceptable for small, globular proteins. Changes much larger than that, however, indicate that the protein is undergoing a large conformational change during the simulation. It is also important that your simulation converges — the RMSD values stabilize around a fixed value. If the RMSD of the protein is still increasing or decreasing on average at the end of the simulation, then your system has not equilibrated, and your simulation may not be long enough for rigorous analysis.

Ligand RMSD: Ligand RMSD (right Y-axis) indicates how stable the ligand is with respect to the protein and its binding pocket. In the above plot, 'Lig fit Prot' shows the RMSD of a ligand when the protein-ligand complex is first aligned on the protein backbone of the reference and then the RMSD of the ligand heavy atoms is measured. If the values observed are significantly larger than the RMSD of the protein, then it is likely that the ligand has diffused away from its initial binding site.

SCHRÖDINGER.

Protein RMSF

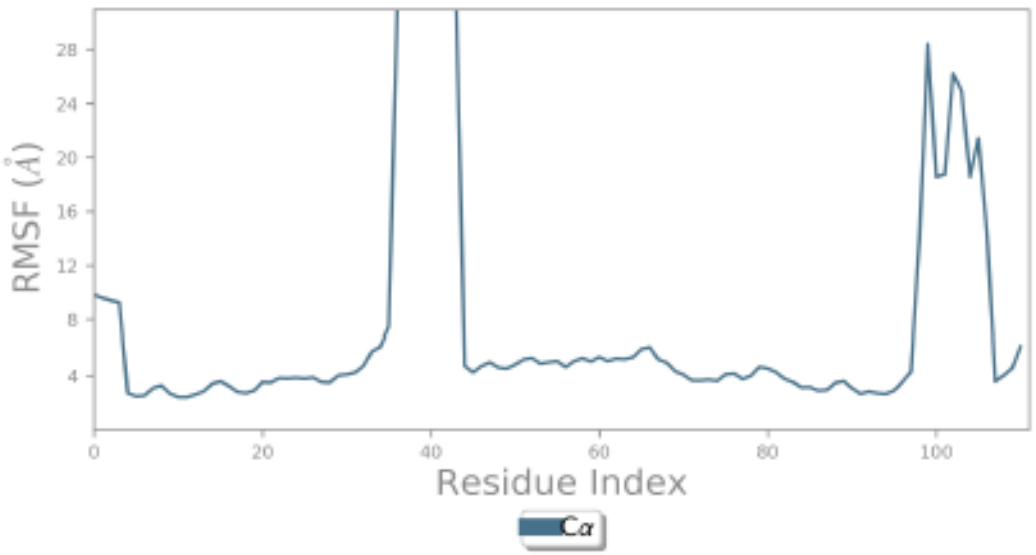

The Root Mean Square Fluctuation (RMSF) is useful for characterizing local changes along the protein chain. The RMSF for residue *i* is:

$$RMSF_i = \sqrt{\frac{1}{T}\sum_{t=1}^{T} < (r'_i(t) - r_i(t_{ref}))^2 >}$$

where *T* is the trajectory time over which the RMSF is calculated, t_{ref} is the reference time, r_i is the position of residue *i*, *r'* is the position of atoms in residue *i* after superposition on the reference, and the angle brackets indicate that the average of the square distance is taken over the selection of atoms in the residue.

On this plot, peaks indicate areas of the protein that fluctuate the most during the simulation. Typically you will observe that the tails (*N*- and *C*-terminal) fluctuate more than any other part of the protein. Secondary structure elements like alpha helices and beta strands are usually more rigid than the unstructured part of the protein, and thus fluctuate less than the loop regions.

SCHRÖDINGER.

Protein Secondary Structure

% Helix	% Strand	% Total SSE
11.93	3.13	15.05

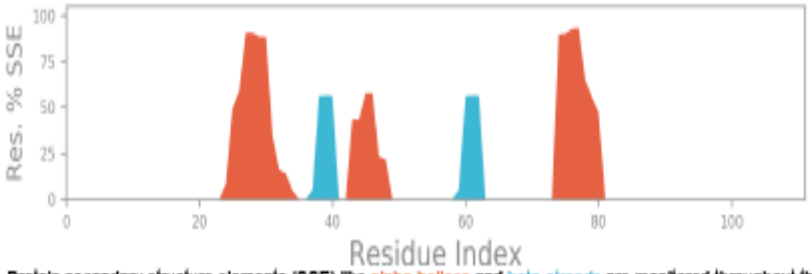

Protein secondary structure elements (SSE) like alpha-helices and beta-strands are monitored throughout the simulation. The plot above reports SSE distribution by residue index throughout the protein structure. The plot below summarizes the SSE composition for each trajectory frame over the course of the simulation, and the plot at the bottom monitors each residue and its SSE assignment over time.

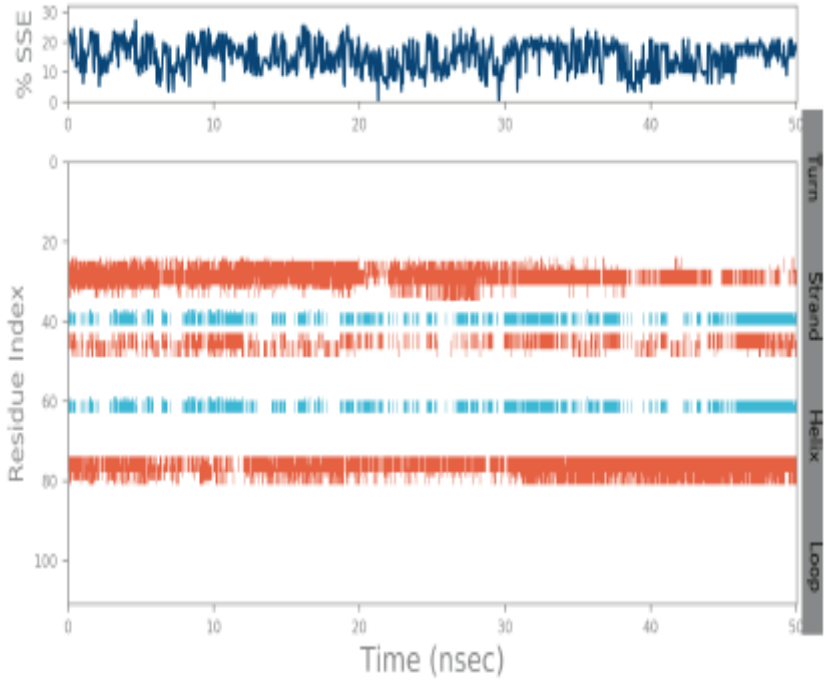

SCHRÖDINGER.

Ligand RMSF

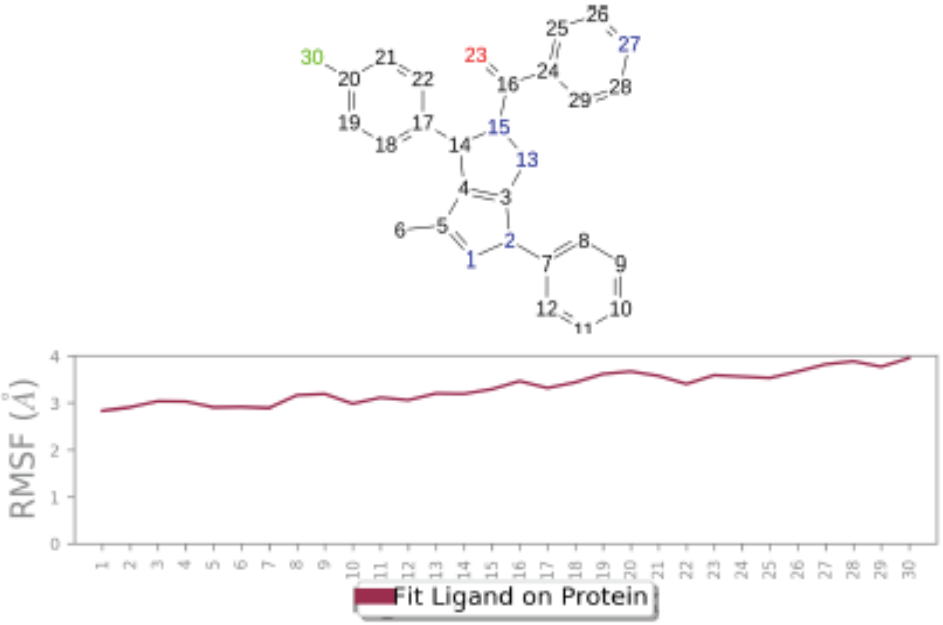

The Ligand Root Mean Square Fluctuation (L-RMSF) is useful for characterizing changes in the ligand atom positions. The RMSF for atom *i* is:

$$RMSF_i = \sqrt{\frac{1}{T}\sum_{t=1}^{T}(r_i'(t) - r_i(t_{ref}))^2}$$

where *T* is the trajectory time over which the RMSF is calculated, t_{ref} is the reference time (usually for the first frame, and is regarded as the zero of time); *r* is the position of atom *i* in the reference at time t_{ref}, and *r'* is the position of atom *i* at time *t* after superposition on the reference frame.

Ligand RMSF shows the ligand's fluctuations broken down by atom, corresponding to the 2D structure in the top panel. The ligand RMSF may give you insights on how ligand fragments interact with the protein and their entropic role in the binding event. In the bottom panel, the 'Fit Ligand on Protein' line shows the ligand fluctuations, with respect to the protein. The protein-ligand complex is first aligned on the protein backbone and then the ligand RMSF is measured on the ligand heavy atoms.

Protein-Ligand Contacts

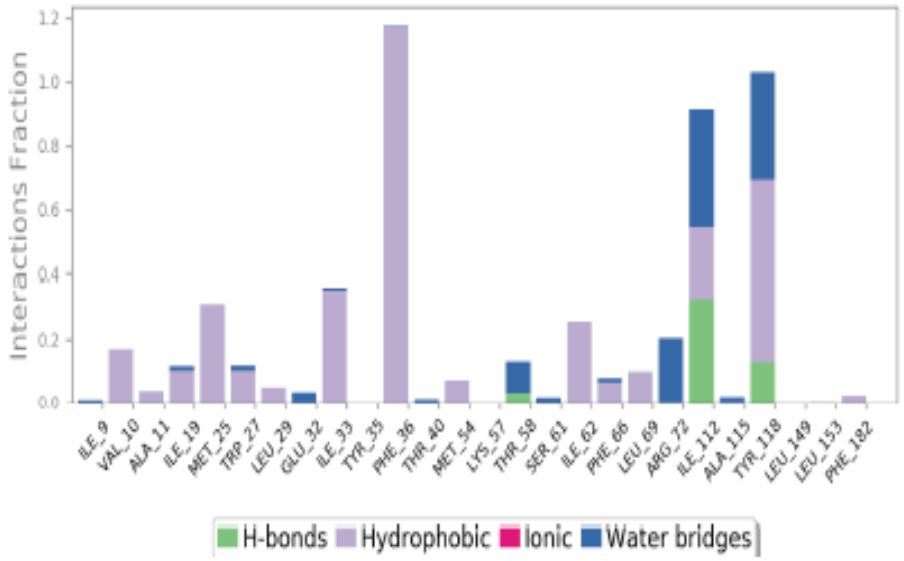

Protein interactions with the ligand can be monitored throughout the simulation. These interactions can be categorized by type and summarized, as shown in the plot above. Protein-ligand interactions (or 'contacts') are categorized into four types: Hydrogen Bonds, Hydrophobic, Ionic and Water Bridges. Each interaction type contains more specific subtypes, which can be explored through the 'Simulation Interactions Diagram' panel. The stacked bar charts are normalized over the course of the trajectory: for example, a value of 0.7 suggests that 70% of the simulation time the specific interaction is maintained. Values over 1.0 are possible as some protein residue may make multiple contacts of same subtype with the ligand.

Hydrogen Bonds: (H-bonds) play a significant role in ligand binding. Consideration of hydrogen-bonding properties in drug design is important because of their strong influence on drug specificity, metabolization and adsorption. Hydrogen bonds between a protein and a ligand can be further broken down into four subtypes: backbone acceptor; backbone donor; side-chain acceptor; side-chain donor.
The current geometric criteria for protein-ligand H-bond is: distance of 2.5 Å between the donor and acceptor atoms (D—H···A); a donor angle of ≥120° between the donor-hydrogen-acceptor atoms (D—H···A); and an acceptor angle of ≥90° between the hydrogen-acceptor-bonded_atom atoms (H···A—X).

Hydrophobic contacts: fall into three subtypes: π-Cation; π-π; and Other, non-specific interactions. Generally these type of interactions involve a hydrophobic amino acid and an aromatic or aliphatic group on the ligand, but we have extended this category to also include π-Cation interactions.
The current geometric criteria for hydrophobic interactions is as follows: π-Cation — Aromatic and charged groups within 4.5 Å; π-π — Two aromatic groups stacked face-to-face or face-to-edge; Other — A non-specific hydrophobic sidechain within 3.6 Å of a ligand's aromatic or aliphatic carbons.

Ionic Interactions: or polar interactions, are between two oppositely charged atoms that are within 3.7 Å of each other and do not involve a hydrogen bond. We also monitor Protein-Metal-Ligand interactions, which are defined by a metal ion coordinated within 3.4 Å of protein's and ligand's heavy atoms (except carbon). All ionic interactions are broken down into two subtypes: those mediated by a protein backbone or side chains.

Water Bridges: are hydrogen-bonded protein-ligand interactions mediated by a water molecule. The hydrogen-bond geometry is slightly relaxed from the standard H-bond definition.
The current geometric criteria for a protein-water or water-ligand H-bond are: a distance of 2.8 Å between the donor and acceptor atoms (D—H···A); a donor angle of ≥110° between the donor-hydrogen-acceptor atoms (D—H···A); and an acceptor angle of ≥90° between the hydrogen-acceptor-bonded_atom atoms (H···A—X).

SCHRÖDINGER.

Protein-Ligand Contacts (cont.)

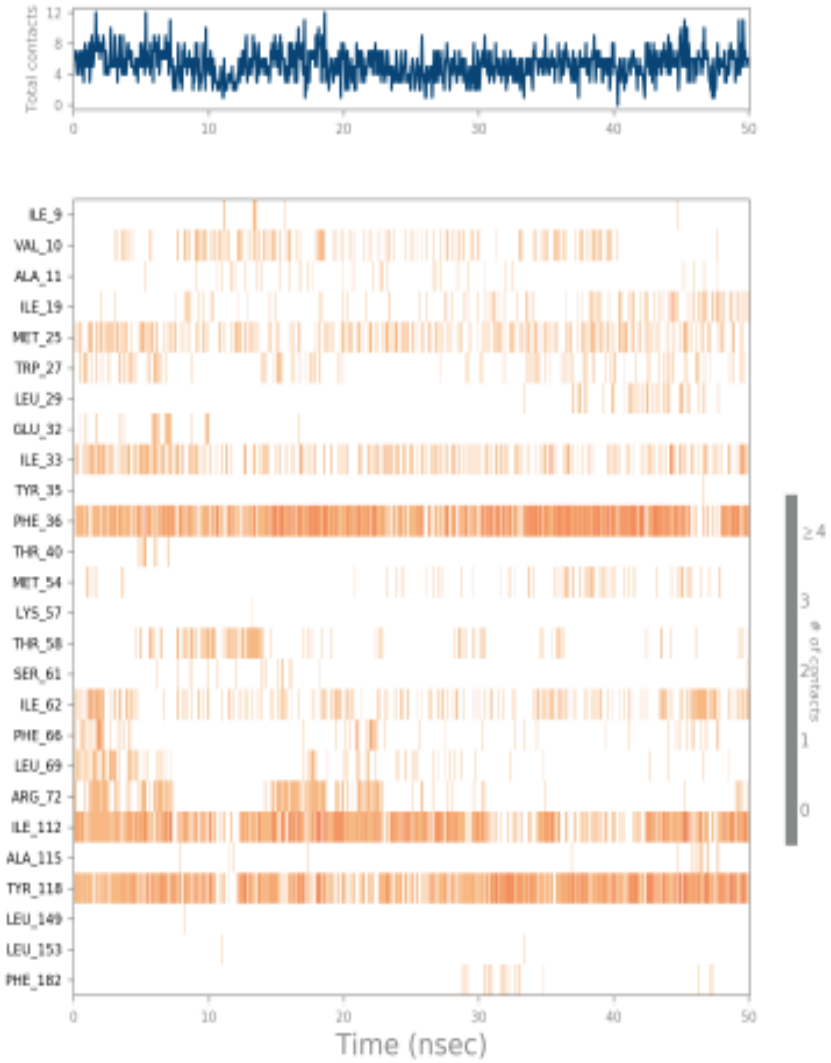

A timeline representation of the interactions and contacts (H-bonds, Hydrophobic, Ionic, Water bridges) summarized in the previous page. The top panel shows the total number of specific contacts the protein makes with the ligand over the course of the trajectory. The bottom panel shows which residues interact with the ligand in each trajectory frame. Some residues make more than one specific contact with the ligand, which is represented by a darker shade of orange, according to the scale to the right of the plot.

SCHRÖDINGER.

Ligand-Protein Contacts

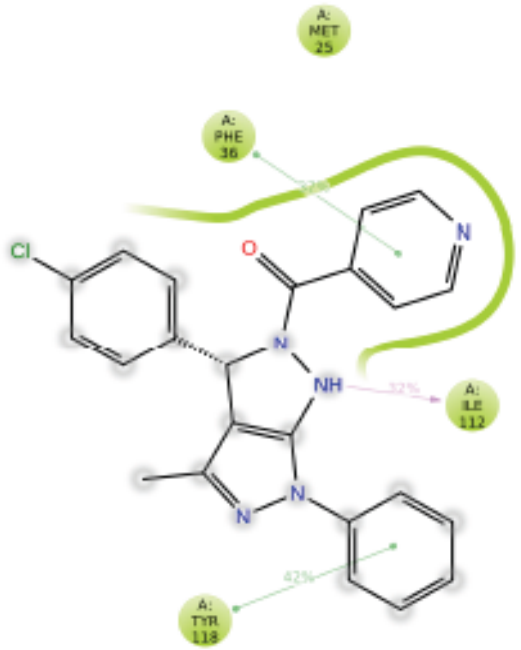

Hydrophobic Pi-Pi stacking Solvent exposure

A schematic of detailed ligand atom interactions with the protein residues. Interactions that occur more than 30.0% of the simulation time in the selected trajectory (0.00 through 50.05 nsec), are shown.
Note: it is possible to have interactions with >100% as some residues may have multiple interactions of a single type with the same ligand atom. For example, the ARG side chain has four H-bond donors that can all hydrogen-bond to a single H-bond acceptor.

Ligand Torsion Profile

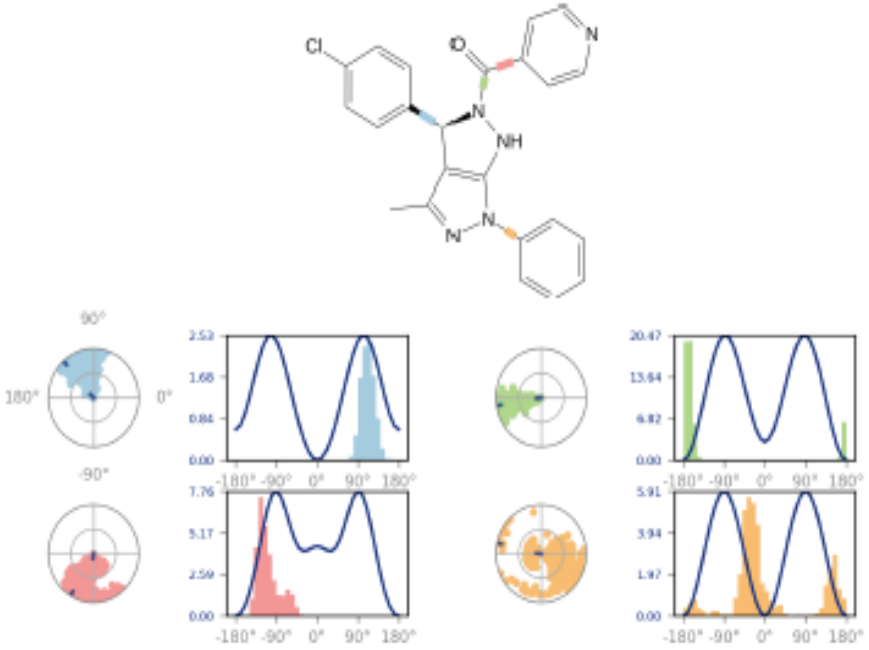

The ligand torsions plot summarizes the conformational evolution of every rotatable bond (RB) in the ligand throughout the simulation trajectory (0.00 through 50.05 nsec). The top panel shows the 2d schematic of a ligand with color-coded rotatable bonds. Each rotatable bond torsion is accompanied by a dial plot and bar plots of the same color.

Dial (or radial) plots describe the conformation of the torsion throughout the course of the simulation. The beginning of the simulation is in the center of the radial plot and the time evolution is plotted radially outwards.

The bar plots summarize the data on the dial plots, by showing the probability density of the torsion. If torsional potential information is available, the plot also shows the potential of the rotatable bond (by summing the potential of the related torsions). The values of the potential are on the left *Y*-axis of the chart, and are expressed in *kcal/mol*. Looking at the histogram and torsion potential relationships may give insights into the conformational strain the ligand undergoes to maintain a protein-bound conformation.

SCHRÖDINGER.

Ligand Properties

Ligand RMSD: Root mean square deviation of a ligand with respect to the reference conformation (typically the first frame is used as the reference and it is regarded as time *t*=0).

Radius of Gyration (rGyr): Measures the 'extendedness' of a ligand, and is equivalent to its principal moment of inertia.

Intramolecular Hydrogen Bonds (intraHB): Number of internal hydrogen bonds (HB) within a ligand molecule.

Molecular Surface Area (MolSA): Molecular surface calculation with 1.4 Å probe radius. This value is equivalent to a van der Waals surface area.

Solvent Accessible Surface Area (SASA): Surface area of a molecule accessible by a water molecule.

Polar Surface Area (PSA): Solvent accessible surface area in a molecule contributed only by oxygen and nitrogen atoms.

Molecular dynamics simulations for compound 1g

SCHRÖDINGER.

Simulation Interactions Diagram Report

Simulation Details

Jobname: **desmond_md_job_1**
Entry title: **Full System**

CPU #	Job Type	Ensemble	Temp. [K]	Sim. Time [ns]	# Atoms	# Waters	Charge
1	mdsim	NPT	300.0	50.096	16064	4755	0

Protein Information

Tot. Residues	Prot. Chain(s)	Res. in Chain(s)	# Atoms	# Heavy Atoms	Charge
112	'A'	112	1709	834	-3

Ligand Information

SMILES	CC(C)=CCC/C(C)=C\[C@@H]1N(C(=O)c2ccncc2)Nc(c13)n(nc3C)-c4ccccc4
PDB Name	'UNK'
Num. of Atoms	61 (total) 32 (heavy)
Atomic Mass	427.554 au
Charge	0
Mol. Formula	C26H29N5O
Num. of Fragments	4
Num. of Rot. Bonds	7

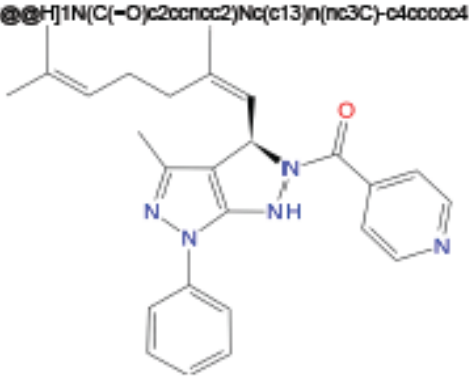

Counter Ion/Salt Information

Type	Num.	Concentration [mM]	Total Charge
Na	16	61.180	+16
Cl	13	49.706	-13

SCHRÖDINGER.

Protein-Ligand RMSD

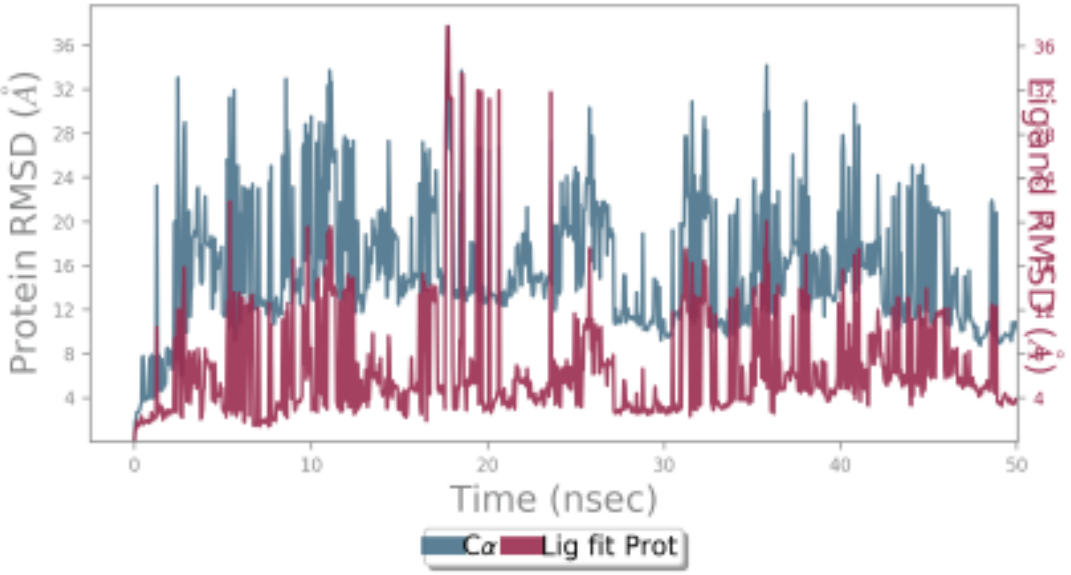

The Root Mean Square Deviation (RMSD) is used to measure the average change in displacement of a selection of atoms for a particular frame with respect to a reference frame. It is calculated for all frames in the trajectory. The RMSD for frame *x* is:

$$RMSD_x = \sqrt{\frac{1}{N}\sum_{i=1}^{N}(r_i'(t_x) - r_i(t_{ref}))^2}$$

where *N* is the number of atoms in the atom selection; t_{ref} is the reference time, (typically the first frame is used as the reference and it is regarded as time *t*=0); and *r'* is the position of the selected atoms in frame *x* after superimposing on the reference frame, where frame *x* is recorded at time t_x. The procedure is repeated for every frame in the simulation trajectory.

Protein RMSD: The above plot shows the RMSD evolution of a protein (left Y-axis). All protein frames are first aligned on the reference frame backbone, and then the RMSD is calculated based on the atom selection. Monitoring the RMSD of the protein can give insights into its structural conformation throughout the simulation. RMSD analysis can indicate if the simulation has equilibrated — its fluctuations towards the end of the simulation are around some thermal average structure. Changes of the order of 1-3 Å are perfectly acceptable for small, globular proteins. Changes much larger than that, however, indicate that the protein is undergoing a large conformational change during the simulation. It is also important that your simulation converges — the RMSD values stabilize around a fixed value. If the RMSD of the protein is still increasing or decreasing on average at the end of the simulation, then your system has not equilibrated, and your simulation may not be long enough for rigorous analysis.

Ligand RMSD: Ligand RMSD (right Y-axis) indicates how stable the ligand is with respect to the protein and its binding pocket. In the above plot, 'Lig fit Prot' shows the RMSD of a ligand when the protein-ligand complex is first aligned on the protein backbone of the reference and then the RMSD of the ligand heavy atoms is measured. If the values observed are significantly larger than the RMSD of the protein, then it is likely that the ligand has diffused away from its initial binding site.

SCHRÖDINGER.

Protein RMSF

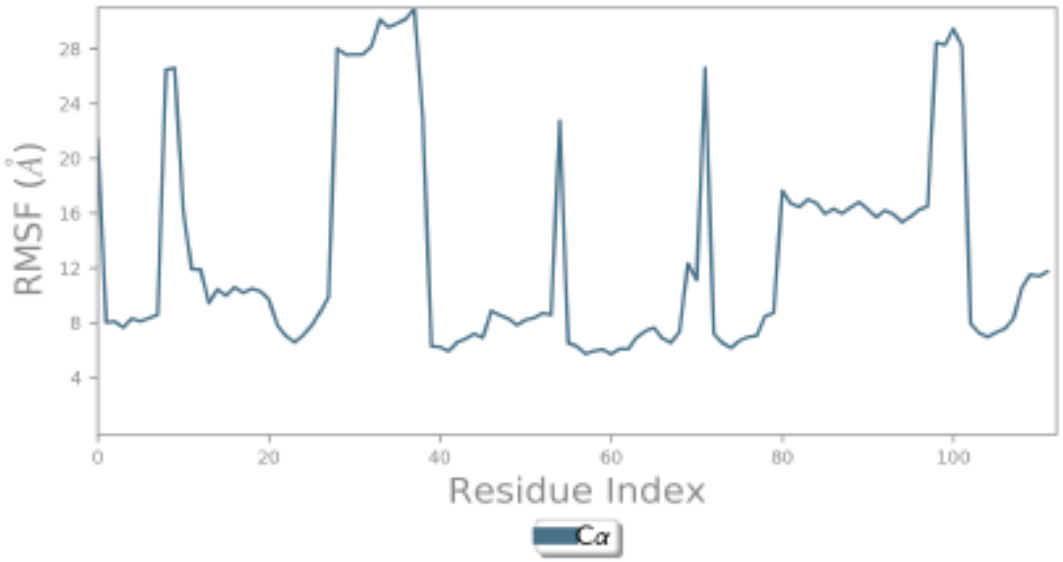

The Root Mean Square Fluctuation (RMSF) is useful for characterizing local changes along the protein chain. The RMSF for residue *i* is:

$$RMSF_i = \sqrt{\frac{1}{T}\sum_{t=1}^{T} < (r_i'(t) - r_i(t_{ref}))^2 >}$$

where *T* is the trajectory time over which the RMSF is calculated, t_{ref} is the reference time, r_i is the position of residue *i*, *r'* is the position of atoms in residue *i* after superposition on the reference, and the angle brackets indicate that the average of the square distance is taken over the selection of atoms in the residue.

On this plot, peaks indicate areas of the protein that fluctuate the most during the simulation. Typically you will observe that the tails (*N*- and *C*-terminal) fluctuate more than any other part of the protein. Secondary structure elements like alpha helices and beta strands are usually more rigid than the unstructured part of the protein, and thus fluctuate less than the loop regions.

SCHRÖDINGER.

Protein Secondary Structure

% Helix	% Strand	% Total SSE
9.15	0.00	9.15

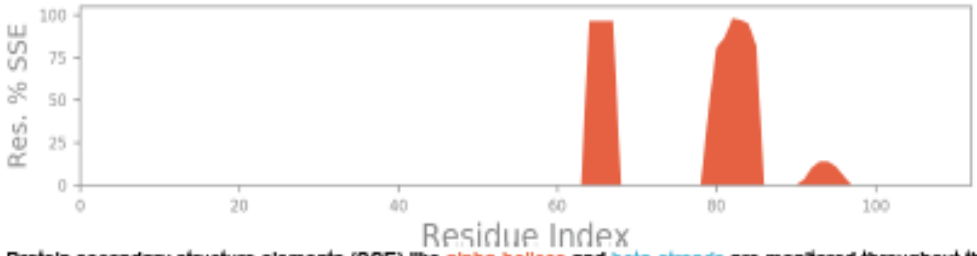

Protein secondary structure elements (SSE) like alpha-helices and beta-strands are monitored throughout the simulation. The plot above reports SSE distribution by residue index throughout the protein structure. The plot below summarizes the SSE composition for each trajectory frame over the course of the simulation, and the plot at the bottom monitors each residue and its SSE assignment over time.

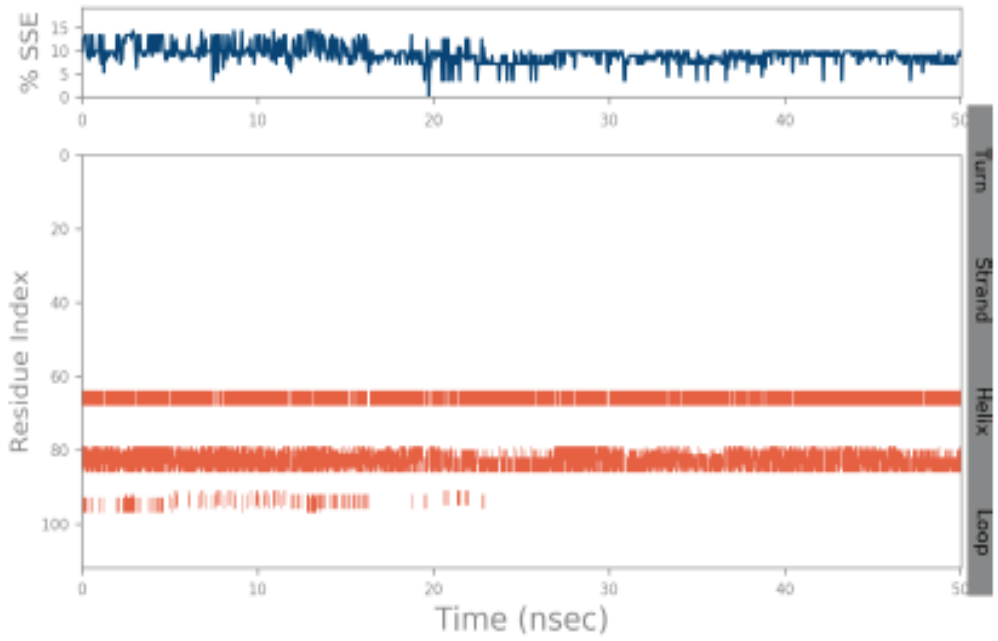

SCHRÖDINGER.

Ligand RMSF

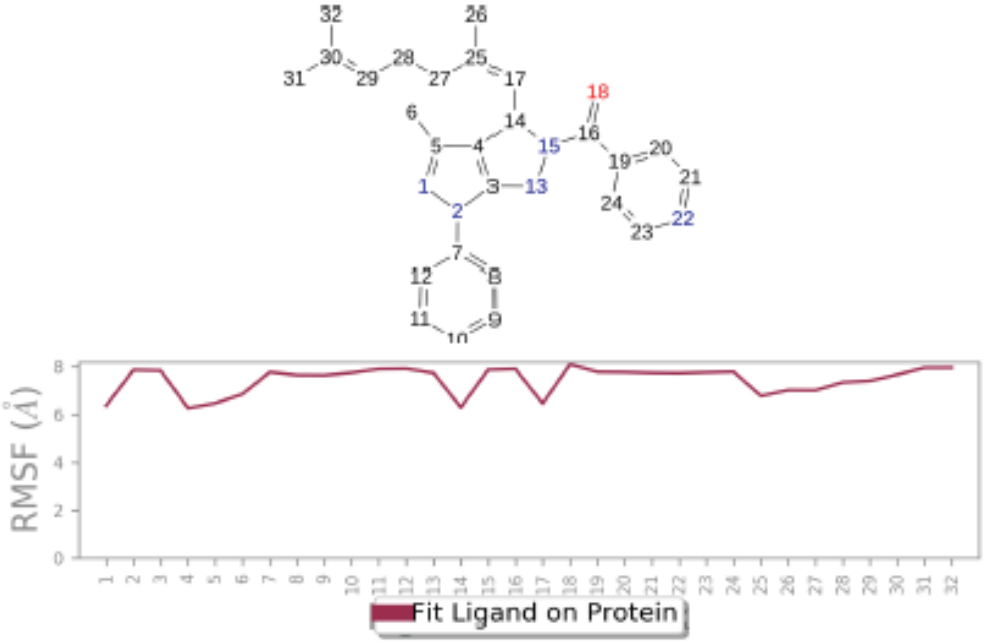

The Ligand Root Mean Square Fluctuation (L-RMSF) is useful for characterizing changes in the ligand atom positions. The RMSF for atom *i* is:

$$RMSF_i = \sqrt{\frac{1}{T}\sum_{t=1}^{T}(r_i'(t) - r_i(t_{ref}))^2}$$

where *T* is the trajectory time over which the RMSF is calculated, t_{ref} is the reference time (usually for the first frame, and is regarded as the *zero* of time); *r* is the position of atom *i* in the reference at time t_{ref} and *r'* is the position of atom *i* at time *t* after superposition on the reference frame.

Ligand RMSF shows the ligand's fluctuations broken down by atom, corresponding to the 2D structure in the top panel. The ligand RMSF may give you insights on how ligand fragments interact with the protein and their entropic role in the binding event. In the bottom panel, the 'Fit Ligand on Protein' line shows the ligand fluctuations, with respect to the protein. The protein-ligand complex is first aligned on the protein backbone and then the ligand RMSF is measured on the ligand heavy atoms.

SCHRÖDINGER.

Protein-Ligand Contacts

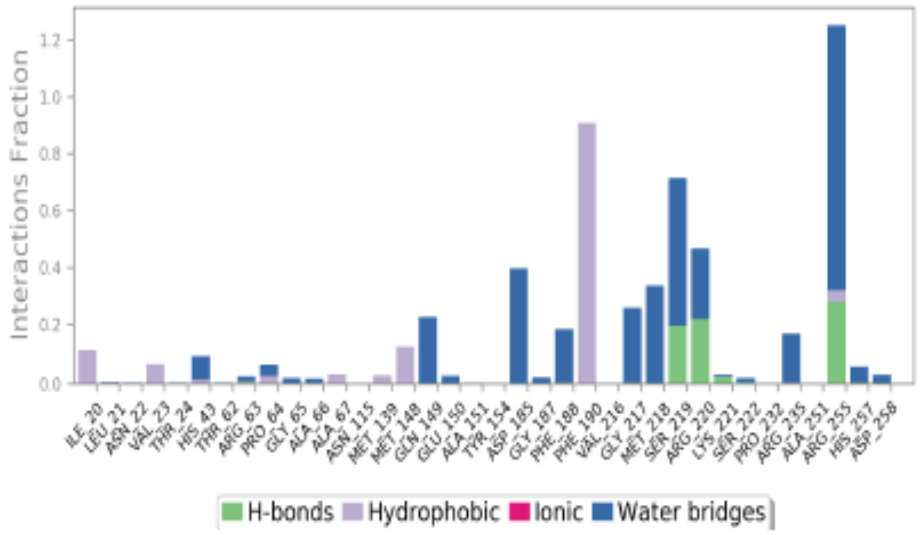

Protein interactions with the ligand can be monitored throughout the simulation. These interactions can be categorized by type and summarized, as shown in the plot above. Protein-ligand interactions (or "contacts") are categorized into four types: Hydrogen Bonds, Hydrophobic, Ionic and Water Bridges. Each interaction type contains more specific subtypes, which can be explored through the 'Simulation Interactions Diagram' panel. The stacked bar charts are normalized over the course of the trajectory: for example, a value of 0.7 suggests that 70% of the simulation time the specific interaction is maintained. Values over 1.0 are possible as some protein residue may make multiple contacts of same subtype with the ligand.

Hydrogen Bonds: (H-bonds) play a significant role in ligand binding. Consideration of hydrogen-bonding properties in drug design is important because of their strong influence on drug specificity, metabolization and adsorption. Hydrogen bonds between a protein and a ligand can be further broken down into four subtypes: backbone acceptor; backbone donor; side-chain acceptor; side-chain donor.
The current geometric criteria for protein-ligand H-bond is: distance of 2.5 Å between the donor and acceptor atoms (D—H···A); a donor angle of ≥120° between the donor-hydrogen-acceptor atoms (D—H···A); and an acceptor angle of ≥90° between the hydrogen-acceptor-bonded_atom atoms (H···A—X).

Hydrophobic contacts: fall into three subtypes: π-Cation; π-π; and Other, non-specific interactions. Generally these type of interactions involve a hydrophobic amino acid and an aromatic or aliphatic group on the ligand, but we have extended this category to also include π-Cation interactions.
The current geometric criteria for hydrophobic interactions is as follows: π-Cation — Aromatic and charged groups within 4.5 Å; π-π — Two aromatic groups stacked face-to-face or face-to-edge; Other — A non-specific hydrophobic sidechain within 3.6 Å of a ligand's aromatic or aliphatic carbons.

Ionic Interactions: or polar interactions, are between two oppositely charged atoms that are within 3.7 Å of each other and do not involve a hydrogen bond. We also monitor Protein-Metal-Ligand interactions, which are defined by a metal ion coordinated within 3.4 Å of protein's and ligand's heavy atoms (except carbon). All Ionic interactions are broken down into two subtypes: those mediated by a protein backbone or side chains.

Water Bridges: are hydrogen-bonded protein-ligand interactions mediated by a water molecule. The hydrogen-bond geometry is slightly relaxed from the standard H-bond definition.
The current geometric criteria for a protein-water or water-ligand H-bond are: a distance of 2.8 Å between the donor and acceptor atoms (D—H···A); a donor angle of ≥110° between the donor-hydrogen-acceptor atoms (D—H···A); and an acceptor angle of ≥90° between the hydrogen-acceptor-bonded_atom atoms (H···A—X).

SCHRÖDINGER.

Protein-Ligand Contacts (cont.)

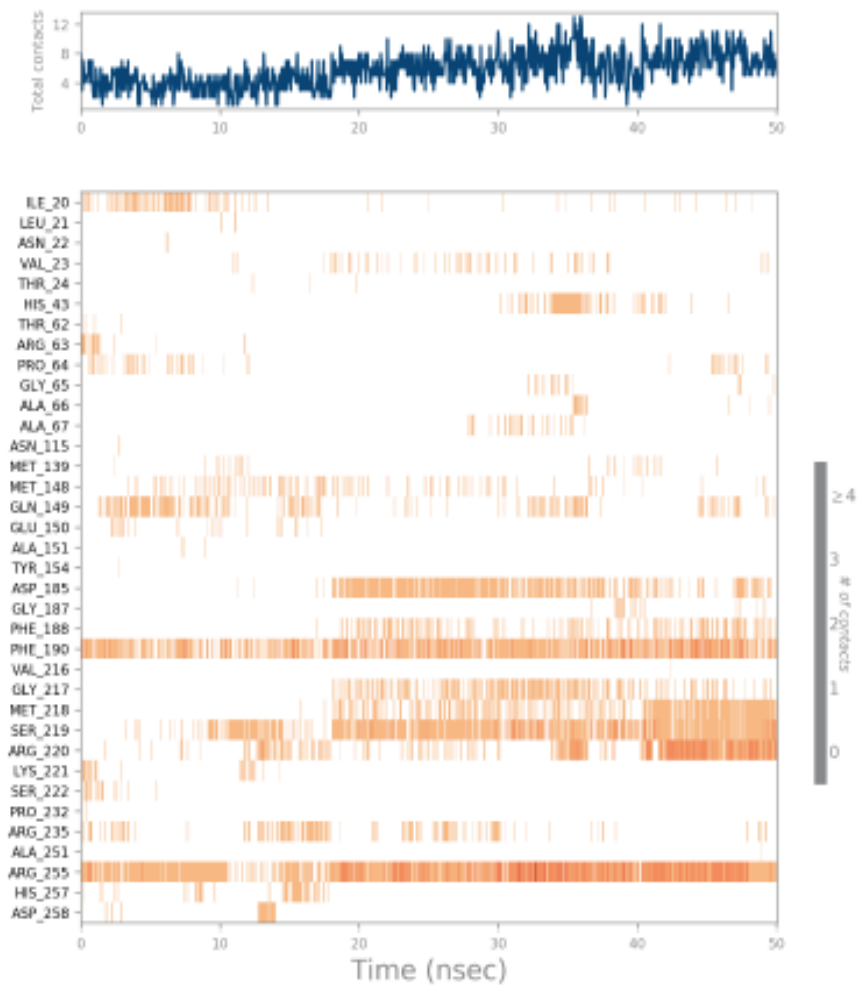

A timeline representation of the interactions and contacts (H-bonds, Hydrophobic, Ionic, Water bridges) summarized in the previous page. The top panel shows the total number of specific contacts the protein makes with the ligand over the course of the trajectory. The bottom panel shows which residues interact with the ligand in each trajectory frame. Some residues make more than one specific contact with the ligand, which is represented by a darker shade of orange, according to the scale to the right of the plot.

SCHRÖDINGER.

Ligand-Protein Contacts

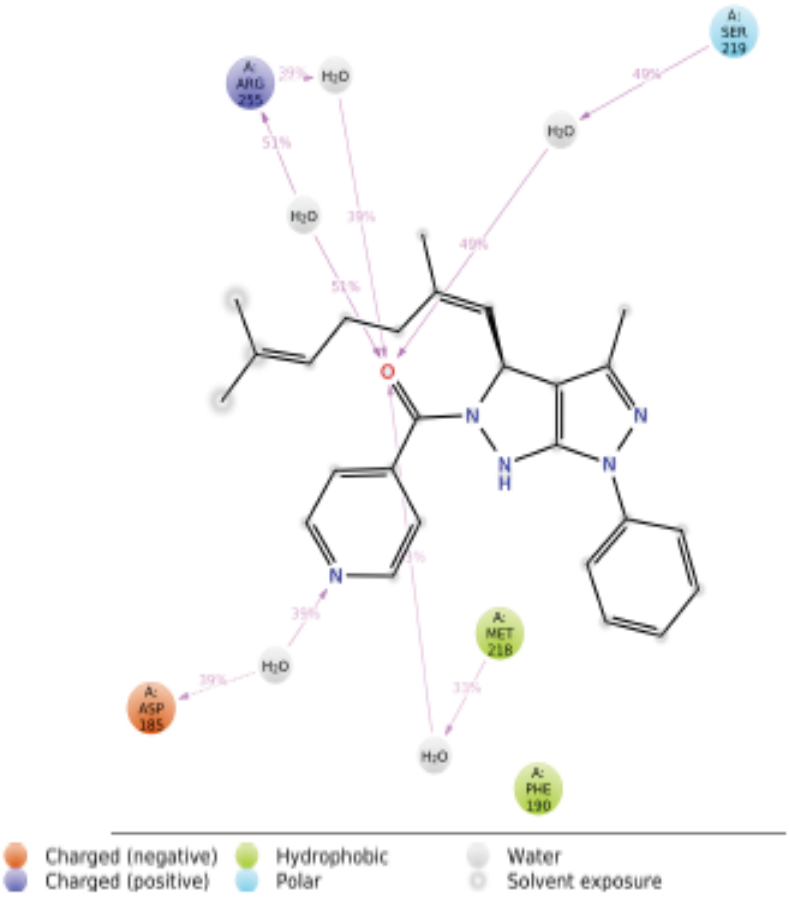

A schematic of detailed ligand atom interactions with the protein residues. Interactions that occur more than 30.0% of the simulation time in the selected trajectory (0.00 through 50.05 nsec), are shown.
Note: it is possible to have interactions with >100% as some residues may have multiple interactions of a single type with the same ligand atom. For example, the ARG side chain has four H-bond donors that can all hydrogen-bond to a single H-bond acceptor.

SCHRÖDINGER.

Ligand Torsion Profile

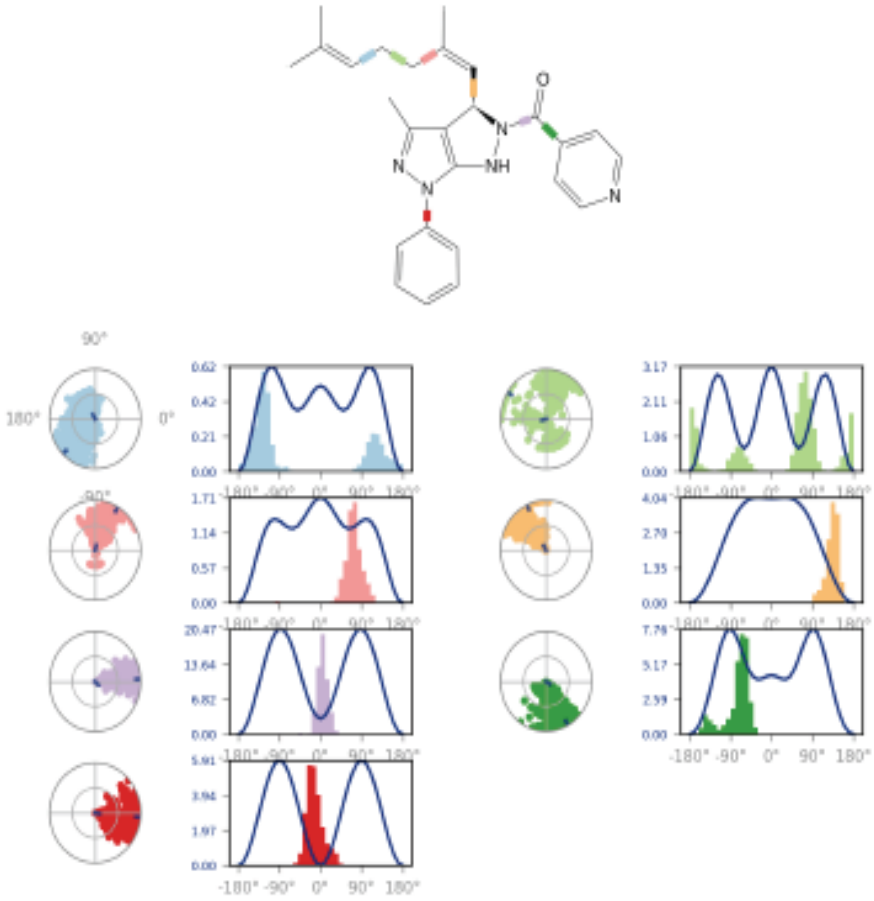

The ligand torsions plot summarizes the conformational evolution of every rotatable bond (RB) in the ligand throughout the simulation trajectory (0.00 through 50.05 nsec). The top panel shows the 2d schematic of a ligand with color-coded rotatable bonds. Each rotatable bond torsion is accompanied by a dial plot and bar plots of the same color.

Dial (or radial) plots describe the conformation of the torsion throughout the course of the simulation. The beginning of the simulation is in the center of the radial plot and the time evolution is plotted radially outwards.

The bar plots summarize the data on the dial plots, by showing the probability density of the torsion. If torsional potential information is available, the plot also shows the potential of the rotatable bond (by summing the potential of the related torsions). The values of the potential are on the left Y-axis of the chart, and are expressed in *kcal/mol*. Looking at the histogram and torsion potential relationships may give insights into the conformational strain the ligand undergoes to maintain a protein-bound conformation.

SCHRÖDINGER.

Ligand Properties

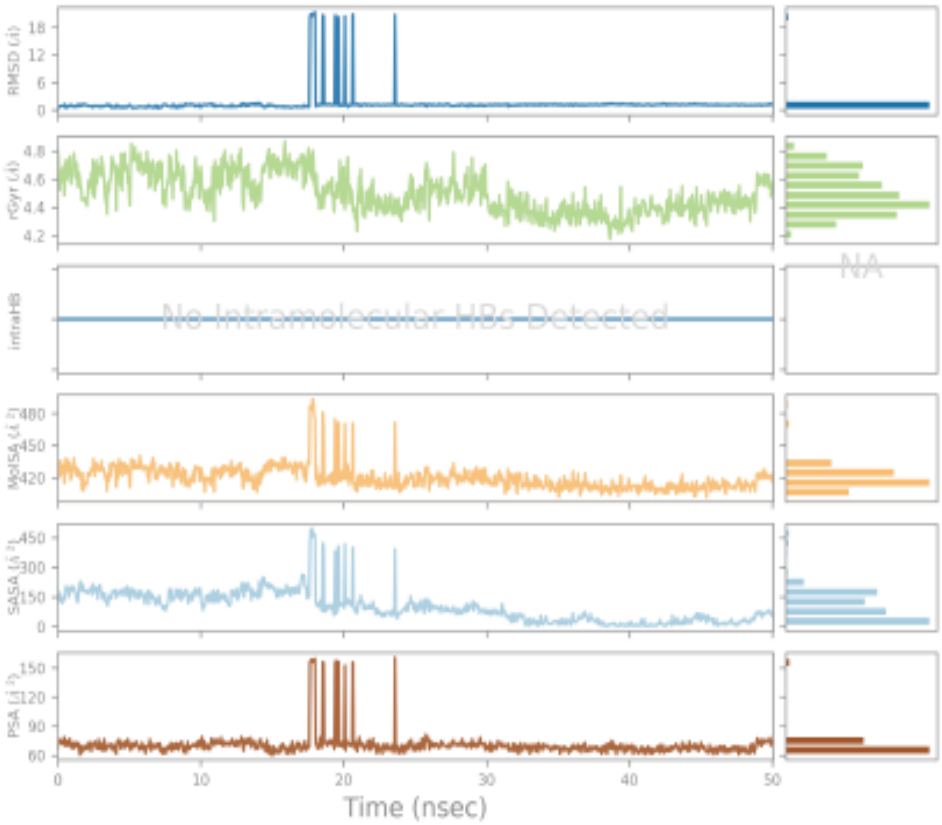

Ligand RMSD: Root mean square deviation of a ligand with respect to the reference conformation (typically the first frame is used as the reference and it is regarded as time *t*=0).

Radius of Gyration (rGyr): Measures the 'extendedness' of a ligand, and is equivalent to its principal moment of inertia.

Intramolecular Hydrogen Bonds (intraHB): Number of internal hydrogen bonds (HB) within a ligand molecule.

Molecular Surface Area (MolSA): Molecular surface calculation with 1.4 Å probe radius. This value is equivalent to a van der Waals surface area.

Solvent Accessible Surface Area (SASA): Surface area of a molecule accessible by a water molecule.

Polar Surface Area (PSA): Solvent accessible surface area in a molecule contributed only by oxygen and nitrogen atoms.